AGU
ADVANCING
EARTH AND
SPACE SCIENCES

JGR Biogeosciences

Key Points:
- We present the first projection of the future marine circulation and biogeochemistry of the Ascension Island Marine Protected Area (AIMPA)
- The AIMPA will become warmer, more saline, more acidic, with less surface nutrients, primary production and chlorophyll
- The AIMPA's capacity to provide ecosystem services will be significantly negatively impacted under a high emission scenario

Correspondence to:
L. de Mora,
ledm@pml.ac.uk

Impacts of Climate Change on the Ascension Island Marine Protected Area and Its Ecosystem Services

L. de Mora[1] , G. Galli[1,2], Y. Artioli[1] , S. Broszeit[1], S. L. Garrard[1] , D. Baum[3], S. Weber[4], and J. Blackford[1]

[1]Plymouth Marine Laboratory, Plymouth, UK, [2]National Institute of Oceanography and Experimental Geophysics, Trieste, Italy, [3]Ascension Island Government, Georgetown, UK, [4]Centre for Ecology and Conservation, University of Exeter, Penryn, UK

Abstract This is the first projection of marine circulation and biogeochemistry for the Ascension Island Marine Protected Area (AIMPA). Marine Protected Areas are a key management tool used to safeguard biodiversity, but their efficacy is increasingly threatened by climate change. To assess an MPA's vulnerability to climate change and predict biological responses, we must first project how the local marine environment will change. We present the projections of an ensemble from the Sixth Coupled Model Intercomparision Project. Relative to the recent past (2000–2010), the multi-model means of the mid-century (2040–2050) project that the AIMPA will become warmer (+0.9 to +1.2°C), more saline (+0.01 to +0.10), with a shallower mixed layer depth (−1.3 to −0.8 m), a weaker Atlantic Equatorial Undercurrent (AEU) (−1.5 to −0.4 Sv), more acidic (−0.10 to −0.07), with lower surface nutrient concentrations (−0.023 to −0.0141 mmol N m^{-3} and −0.013 to −0.009 mmol P m^{-3}), less chlorophyll (−6 to −3 µg m^{-3}) and less primary production (−0.31 to −0.20 mol m^{-2} yr^{-1}). These changes are often more extreme in the scenarios with higher greenhouse gases emissions and more significant climate change. Using the multi-model mean for two scenarios in the years 2090–2100, we assessed how five key ecosystem services in both the shallow subtidal and the pelagic zone were likely to be impacted by climate change. Both low and high emission scenarios project significant changes to the AIMPA, and it is likely that the provision of several ecosystem services will be negatively impacted.

Plain Language Summary Ascension Island is a small remote volcanic island in the equatorial Atlantic Ocean. The seas around Ascension Island have been protected from commercial fishing since 2019. We used the marine component of computer simulations of the Earth's climate to try to understand the future of the Ascension Island Marine Protected Area (AIMPA). Over the next century, the AIMPA region will become warmer, more saline, more acidic, less productive, and with lower nutrient and chlorophyll concentrations in the surface waters. The most important current of the region, the Atlantic Equatorial Current, is also projected to weaken in all scenarios. These changes are likely to negatively impact the ability of the AIMPA to provide ecosystem services such as healthy ecosystems, fish stocks, the removal of carbon dioxide from the air, and attract tourism. This work is important because it is the first projection of the climate around the AIMPA since it was created, and it has allowed local policymakers to understand how the changing climate is likely to affect their environment and ecosystem services.

1. Introduction

Unsustainable fisheries and anthropogenic climate change rank as the most pervasive drivers of marine biodiversity loss worldwide, threatening to undermine ocean health and human well-being alike (Jaureguiberry et al., 2022). Conservation efforts aimed at curbing these losses often center around the establishment of marine protected areas (MPAs). Notably, there are ambitious global targets proposed to protect at least 30% of the ocean by 2030 (Woodley et al., 2019). While recently created MPAs have expanded the MPA coverage from 2.18% in 2016 (O'Leary et al., 2016), to 2.9% in 2023 (Marine Conservation Institute, 2023), this is still significantly below the 30% target.

Appropriately managed and enforced MPAs have proven to be highly effective in reducing and reversing fisheries impacts (Sala et al., 2021). Beyond their benefits to ecosystem health, MPAs have multiple socioeconomic benefits. Even small reserves can increase the abundances of local fishing stock (Hansen et al., 2011), and can also improve local social capital (Maina et al., 2011). Large scale remote marine wilderness MPAs can host several

Writing – original draft: L. de Mora, G. Galli, Y. Artioli
Writing – review & editing: L. de Mora, G. Galli, Y. Artioli, S. Weber, J. Blackford

times more fish biomass than recently fished MPAs while having a significantly more biodiverse ecosystem community (Graham & McClanahan, 2013).

Unfortunately, even highly-protected MPAs remain vulnerable to extrinsic threats from climate change. Within MPAs, species and habitats are exposed to many of the same climate change induced pressures that affect unprotected areas. These stresses include thermal stress, ocean acidification and altered trophic webs (du Pontavice et al., 2020). The warming associated with continued business-as-usual emissions has the potential to drive habitat and species losses even inside fully protected MPAs (Bruno et al., 2018). Furthermore, as habitats are exposed to climate change, their locations may shift and this pressures species to follow their niche as it moves. However, marine habitat distributions are moving an order of magnitude faster than those on land (Bruno et al., 2018). Given the potential of the changing climate to compromise MPA efficacy, many recent studies have stressed the need to expand MPA coverage, incorporate "climate smart" principles into MPA design and management, while also calling for robust assessments of how local marine environments are likely to change in the future (O'Regan et al., 2021; Tittensor et al., 2019; Wilson et al., 2020; Woodley et al., 2019).

In the global context, the ocean's mean surface temperature is projected to increase by between 0.9 and 2.9°C between the years 1995–2010 and 2081–2100 (Fox-Kemper et al., 2021; Lee et al., 2021). This warming will lead to cascading impacts on ocean physics and biogeochemistry. Empirical data indicates that the upper ocean has become more stably stratified since 1970 over the vast majority of the globe (Eyring et al., 2021). The enhanced stratification results in decreased nutrient availability in surface waters and associated reductions in primary production and faunal biomass (Lotze et al., 2019). There is high confidence that many ocean currents will be impacted by changing wind stress (Richter & Tokinaga, 2022; Weijer et al., 2020). Furthermore, increased water temperatures, greater stratification, and weaker overturning circulation will result in reduced dissolved oxygen concentrations and expansion of biologically impoverished oxygen minimum zones (OMZs) (Breitburg et al., 2018; Stramma et al., 2012). In addition to the changing thermal structure of the ocean, the uptake of anthropogenic CO_2 has driven a significant acidification of the global ocean (Lee et al., 2021).

The cumulative impacts of these changes on marine biodiversity are already being observed in many protected and non-protected areas (Bates et al., 2019; Poloczanska et al., 2016). However, the effects of climate change are far from uniform. Projected changes in ocean temperature and biomass often exhibit latitudinal gradients as well as both fine-scale and basin-scale variation (Lotze et al., 2019; Tebaldi et al., 2021). Ocean circulation patterns are also expected to have complex and variable responses to climate change, with some current systems projected to intensify while others weaken (Richter & Tokinaga, 2022; Weijer et al., 2020). Robust local and regional projections are therefore necessary to predict likely biological responses and assess the vulnerability of individual MPAs (Tittensor et al., 2019). Unfortunately, such local projections are generally lacking, meaning that climate change is often framed in MPA management plans as a nebulous threat, without specific impact assessments or adaptation measures (O'Regan et al., 2021).

For this work, we developed the first climate projection of the Ascension Island Marine Protected Area (AIMPA). The UK overseas territory of Ascension Island is a small volcanic island in the tropical South Atlantic. The AIMPA was designated in 2019 and covers the entirety of the 443,571 km^2 exclusive economic zone (EEZ) surrounding Ascension Island, as shown in Figure 1. The AIMPA is currently the 8th largest protected area of the global ocean (Marine Conservation Institute, 2023) and the AIMPA prohibits all forms of commercial fishing and mining, but permits small scale recreational and sports fishing in inshore waters.

The AIMPA harbours a large concentration of marine biodiversity, including an abundance of megafauna, such as sharks, turtles, tunas, billfish, rays and cetaceans (Thompson et al., 2021; Wirtz et al., 2017). The island is a nesting area for seabirds (S. B. Weber & Weber, 2019) and green turtles (Godley et al., 2001; Hays et al., 2002; Broderick et al., 2006; S. B. Weber et al., 2014). Whilst fish and invertebrate species richness is low with a high level of endemism, fish abundance is high (Barnes, 2017; Brickle et al., 2017). Due to its isolation, the AIMPA's shallow water endemic species are unlikely to be able to migrate to neighboring habitats if conditions were to become unfavourable in the future. The AIMPA Management Plan lists climate change as one of the major remaining threats to biodiversity in the region (Ascension Island Government, 2021a). However, no projection existed before now that could be use to estimate ecological responses.

The AIMPA is part of the Saint Helena, Ascension and Tristan da Cunha British Overseas Territory in the southern Atlantic. Both Saint Helena and Tristan da Cunha also host their own MPAs. The Tristan da Cunha MPA
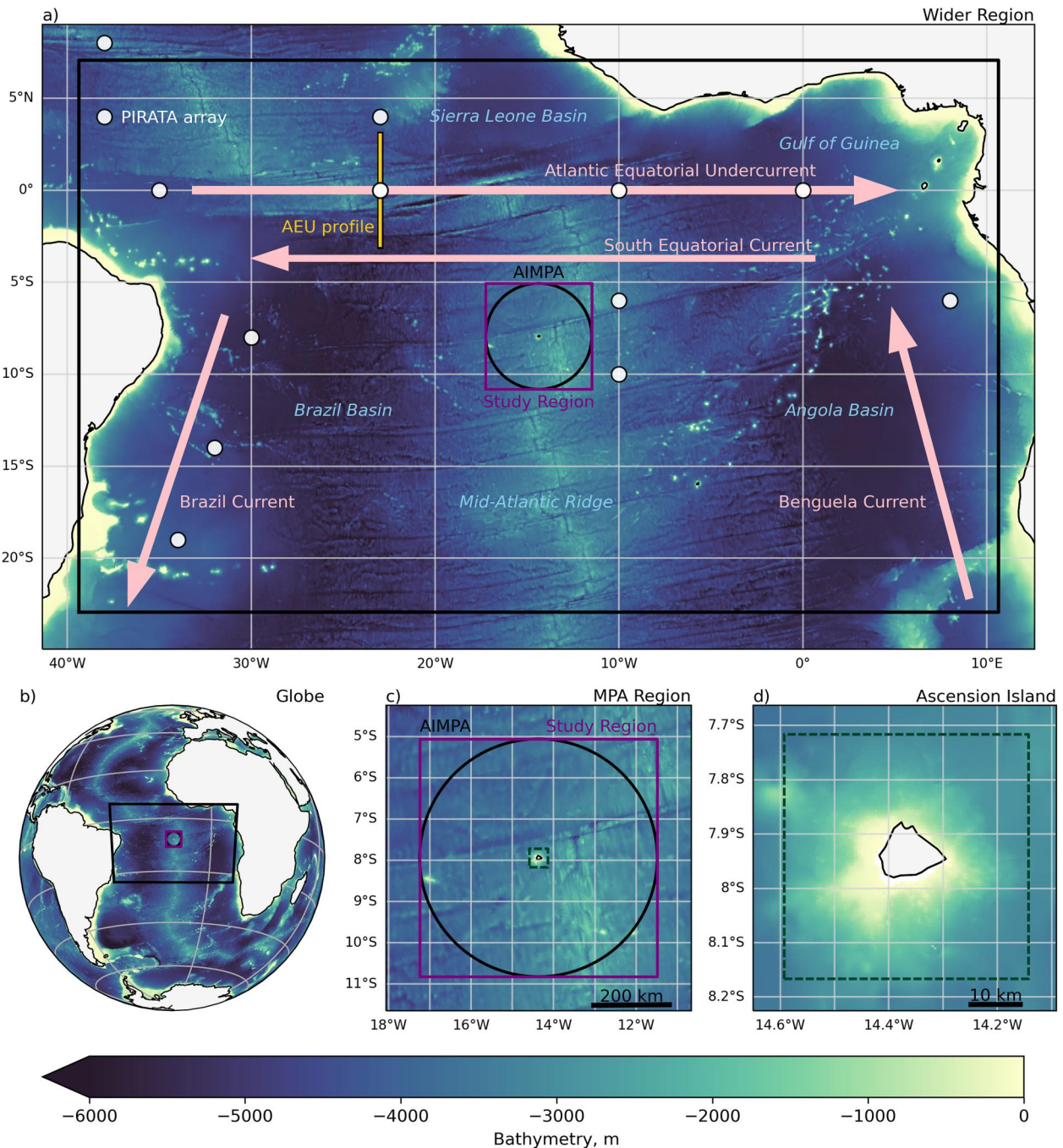
Figure 1. The marine geography around the AIMPA: (a) the wider equatorial Atlantic region, (b) the region and the Ascension Island Marine Protected Area (AIMPA) in a global context, (c) the AIMPA and the study region, (d) a close up of Ascension island. All panes share the same color scale representing the bathymetry. In panel (a), the Atlantic Equatorial Undercurrent (AEU) and several other major currents are shown in light pink, and the major marine regions are labeled in blue italic. Station from the Prediction and Research Moored Array in the Tropical Atlantic (PIRATA) array are shown as white circular markers. The transect line used for the AEU calculation is shown as a north-south yellow line crossing the equator at 28°W. Panes (a, b, c) show the AIMPA region as a black circle and the edges of the study region as a purple square. The bathymetry data shown here is from the General Bathymetric Chart of the Oceans (GEBCO Compilation Group, 2023).

is currently the fifth largest MPA in the ocean (Marine Conservation Institute, 2023). It has a similar protection status to the AIMPA but permits sustainable fishing in its near-shore waters. The entirety of the Saint Helena MPA is a "sustainable use" MPA where marine activities and resource collection are allowed, but managed in a

manner that incorporates cultural values and sustainability (St Helena Goverment, 2023). Together, these MPAs cover 1,578,086 km^2, of which 68% is fully protected (Marine Conservation Institute, 2023).

The work was part of the Climate Resilience And Conservation Of Ascension's Biodiversity (CRACAB) project (S. Weber et al., 2023) and some of these results were previously used to inform Ascension Island Government's strategies and adaptation plans (de Mora et al., 2022). The results shown here are an updated version of that report, including additional model data sets, a more thorough analysis and a revised ecosystem services analysis. The CRACAB project itself used an island-wide approach to generate projections of the most serious impacts of climate change on the Ascension Island and the AIMPA. These projections were then provided to local policymakers and fed into the Ascension Island Government's long term strategy.

We assessed the projection of nine oceanographic properties in the AIMPA over the 21st century using data from the sixth coupled model inter-comparison project Coupled Model Intercomparision Project (CMIP6) (Eyring et al., 2016). The nine oceanographic data sets were temperature, salinity, mixed layer depth (MLD), oxygen concentration, pH, nitrate concentration, phosphate concentration, chlorophyll concentration and integrated primary production (IntPP). The projections covered a range of representative emission scenarios and shared socio-economic pathways. We assessed these data sets in terms of their interannual, climatological, spatial and vertical behaviors.

We subsequently examined how broad-scale ocean circulation patterns in the region could change. We focused specifically on the Atlantic Equatorial Undercurrent (AEU), which has a pervasive influence on the oceanography of the AIMPA (Brandt et al., 2021). The AEU flows eastwards along the equator as shown in Figure 1a with the core of the current at a depth of approximately 80 m. The AEU upwells in the Gulf of Guinea, delivering nutrient rich cooler subsurface water into the westbound Southern Equatorial Current (SEC). This gives rise to a high productivity and low oxygen zone that protrudes westward south of the equator, which can reach the AIMPA. Previous work has reported a weakening of the SEC's cold tongue over recent decades (Tokinaga & Xie, 2011). However, to our knowledge there are few published projections of how the AEU will respond to climate change (Giarolla et al., 2015), and we present the first AEU projection using CMIP6 data.

Finally, we assessed how the projected changes could affect ecosystem service provision in the AIMPA. Ecosystem services are the direct and indirect contributions of ecosystems to human well-being (Sukhdev et al., 2010). Ecosystem services are intrinsically linked to biodiversity in the marine environment (R. T. Watson & Zakri, 2005). Exploitation and climate change are the two most important drivers of marine biodiversity loss (Jaureguiberry et al., 2022), and any decline in biodiversity and hence ecosystem services could jeopardise both marine ecosystems and human well-being in the AIMPA (R. T. Watson & Zakri, 2005).

2. Methods

The methods are described below in five separate subsections. Firstly, in Section 2.1, the CMIP6 framework, the source of the simulated climate data sets, is introduced. Secondly, the nine oceanographic properties that were provided directly in CMIP6 were analyzed using the common framework described in Section 2.2. Then, the AEU analysis methodology and the ecosystem service assessment methodology are described in Sections 2.3 and 2.4. Finally, the hardware and software tools are described in Section 2.5.

2.1. The Sixth Coupled Model Inter-Comparison Project (CMIP6)

The data that were used to generate this analysis were taken from global scale Earth System Models (ESMs) from CMIP6 (Eyring et al., 2016). CMIP6 is an international collaborative project that allows modeling groups from around the world to share and compare their climate model output data sets. CMIP6 represents the state-of-the-art in Earth system modeling, and has a significantly larger volume of data of any previous generation of CMIP (Balaji et al., 2018; Petrie et al., 2021). To participate, models are required to meet predefined scientific model quality and data formatting standards (Eyring et al., 2016; Jones et al., 2011; Yool et al., 2020).

Relative to CMIP5, CMIP6 models have smaller biases in the mean state and variability of the tropical Atlantic, and the equatorial Atlantic sea surface temperature (SST) warm bias and westerly wind bias have both been mostly eliminated in CMIP6 (Richter & Tokinaga, 2022). Furthermore, the seasonal and interannual variabilities of CMIP6 models in the equatorial and subtropical Atlantic compares favorably to those seen in the observations-

Table 1
The Total Number of Contributing Models and the Total Number of Contributing Ensemble Members (Given in Parentheses)

Field	Historical	SSP1-2.6	SSP2-4.5	SSP3-7.0	SSP5-8.5
Temperature	37 (189)	33 (122)	33 (84)	31 (141)	34 (90)
Salinity	25 (135)	23 (79)	23 (70)	21 (87)	24 (77)
MLD	20 (108)	9 (50)	19 (72)	7 (58)	8 (45)
Oxygen	8 (83)	8 (52)	8 (42)	8 (68)	8 (39)
pH	8 (49)	8 (32)	7 (22)	8 (49)	7 (22)
Nitrate	9 (20)	8 (18)	8 (12)	8 (18)	9 (13)
Phosphate	8 (23)	7 (22)	7 (11)	7 (22)	8 (12)
Chlorophyll	8 (58)	7 (41)	7 (36)	7 (48)	8 (35)
Int. PP	14 (39)	11 (34)	11 (35)	12 (35)	8 (12)
AEU	24 (77)	19 (61)	21 (55)	19 (66)	21 (60)

based Climate Reanalysis (Richter & Tokinaga, 2022). This suggests that CMIP6 models should be sufficiently capable of projecting the coarse-scale physical behavior and variability patterns of the AIMPA.

The CMIP6 historical simulations span the years 1850–2014. The forcing data used to drive the climate in the historical scenarios are based on observations, including historic greenhouse gas concentrations, emissions of short-lived and long-lived species of greenhouse gases, global gridded land-use forcing data, solar forcing, and stratospheric aerosol including volcanic output (Eyring et al., 2016). The Scenario Model Intercomparison Project (ScenarioMIP) provides the environmental forcing data required to drive multiple ESM projections of the years 2015–2100. These include several pathways of future social and economic drivers, which result in different atmospheric concentration of greenhouse gases and other climate forcers (O'Neill et al., 2016). In this work, we included the scenarios: SSP1-2.6, SSP2-4.5, SSP3-7.0 and SSP5-8.5, as described in Riahi et al. (2017). These scenarios span a wide range of possible futures, including sustainable development in the SSP1-2.6 scenario. The "middle of the road" pathway is SSP2-4.5, which extrapolates historic and current global development into the future with a medium radiative forcing by the end of the century. The regional rivalry scenario, SSP3-7.0, revives nationalism and regional conflicts, pushing global issues into the background, which results in higher emissions. While the other scenarios approximately scale CO_2 with methane and aerosols, SSP3-7.0 has proportionally higher aerosol (sulfur and black carbon) and methane emissions, driven by a significant decline in forest and natural land coverage and a rise in the land area used as pasture (O'Neill et al., 2016; Riahi et al., 2017). Finally, SSP5-8.5 is a projection designed to include enhanced fossil fuel development and extremely high fossil fuel deployment. SSP5-8.5 has extremely high CO_2 emissions, a rapid decline in aerosols, and constant rise in methane.

In practice, CMIP6 modeling groups generate multiple historical and future simulations, and often more than one simulation per scenario. Each individual simulation is called an ensemble member. Ensemble members for a given model typically have different initial conditions. This is because the precise conditions of the climate at the start of the historical period in 1850 are unknown but may have a significant influence on the evolution of the whole climate system. As such, there is some variability between models in the number of ensemble members generated for each scenario. For instance, while some models contribute only one historical simulation, other models may contribute significantly more. For instance, 19 different historical ensemble members were generated for the UKESM1-0-L model (Sellar et al., 2020). To balance models with many ensemble members against models with fewer ensemble members, the "one model – one vote" weighting scheme is used. This means that each model has equal weight in the multi-model mean (MMM). In practice, each ensemble member is weighted inversely-proportional to the total number of ensemble members that the model contributed to the analysis. The multi-model means were not further weighted in terms of model quality, historical performance, or climate sensitivity.

2.2. CMIP6 Multimodel Analysis (CMA)

A common analysis framework, the CMIP6 Multimodel Analysis (CMA), was used to analyze the following variables in the AIMPA region: temperature, salinity, MLD, oxygen concentration at 500 m, pH, nitrate concentration, phosphate concentration, chlorophyll concentration and IntPP. These are all variables that are directly produced in CMIP6 and can be analyzed without requiring any additional derivation. We required each ensemble member to be available on the British Atmospheric Data Centre (BADC) data storage system and visible from the supercomputer, JASMIN, where the work was carried out as described in Section 2.5. We excluded the ensemble member if the model grid area (`areacello`) data were absent, the time series was incomplete, or the data could not be made compliant with CMIP6 formatting standards. Table 1 shows the number of models and total number of CMIP6 ensemble members for each field for each scenario. Note that CMIP6 has separate data sets for surface-only and depth-resolved temperature (*tos* and *thetao*) and salinity (*sos* and *so*). Table 2 lists the CMIP6 models that contributed to each CMA.

Table 2
The List of Models That Contributed to Each CMA

Model	T	S	MLD	O_2	pH	NO_3	PO_4	Chl	IntPP	AEU
ACCESS-CM2	xxx	xxx	xox							xxx
ACCESS-ESM1-5	xxx	xxx	xox	xxx		xxx	xxx	xxx	xox	xxx
BCC-CSM2-MR	oox									
CAMS-CSM1-0	oox									
CanESM5	xxx	xxx	xox	xxx		xxx		xxx	xox	xxx
CanESM5-CanOE	xox	xxx							xox	
CAS-ESM2-0	xxx	xxx	xox							xxx
CESM2	xox	xxx				xox	xxx	xxx	xox	
CESM2-WACCM	xxx	xxx	xox		xxx				xox	xxx
CIESM	xxx	xxx								xxx
CMCC-CM2-SR5	xxx	xxx	xox							xxx
CMCC-ESM2	xxx	xxx	xox	xxx	xxx	xxx	xxx	xxx	xox	xxx
CNRM-CM6-1	xxx	xxx	xox				xxx	xxx	xox	xxx
CNRM-CM6-1-HR	xox	xxx								
CNRM-ESM2-1	xxx	xxx	xox	xxx	xxx	xxx				xxx
EC-Earth3	xxx	xxx	xox							xxx
EC-Earth3-AerChem	xxx	xxx								xxx
EC-Earth3-CC	xxx	xxx	xox						xox	xxx
EC-Earth3-Veg	oox	xxx	xox							xxx
EC-Earth3-Veg-LR	oxx									xxx
FGOALS-f3-L										xxx
FGOALS-g3										xxx
FIO-ESM-2-0	xxx									xxx
GFDL-CM4	oox									
GFDL-ESM4	oox									
HadGEM3-GC31-LL	xxx	xxx	xox							xxx
HadGEM3-GC31-MM	xxx	oox	xox							xxx
IPSL-CM5A2-INCA	xxx	xxx			xxx				xox	
IPSL-CM6A-LR	xxx		xox	xx	xxx	xxx	xxx	xxx	xox	xxx
MCM-UA-1-0	xxx									
MIROC6	oox	oox	xox							
MPI-ESM-1-2-HAM	xxx								xox	
MPI-ESM1-2-HR	oox	xxx	xox	xxx	xxx				xox	
MPI-ESM1-2-LR	xxx	xxx	xox	xxx	xxx	xxx	xxx		xox	
MRI-ESM2-0	xxx	xxx	xox			xxx	xxx	xxx		xxx
NorESM2-LM	oox									
NorESM2-MM	oox									
TaiESM1	xxx									xxx
UKESM1-0-LL	xxx	xxx	xox	xxx	xxx	xxx	xxx	xxx	xox	xxx

Note. Data contribution is labeled with an "x," and a blank entry or an "o" indicate no data from this model in the analysis. The three "x" or "o" indicate whether model contributed to the time series & climatology, depth profile, and spatial distribution analyses, respectively. The columns are labelled as T: temperature, S: salinity, MLD: mixed layer depth, O_2: oxygen concentration, NO_3: nitrate concentration, PO_4: phosphate concentration, Chl: chlorophyll concentration, IntPP: integrated primary production, and AEU: Atlantic equatorial undercurrent.

Table 3
The Observational Datasets Used in This Analysis and Their References

Field	Dataset	Reference
Temperature	ERA-Interim	Dee et al. (2011)
	WOA	Locarnini et al. (2018)
Salinity	WOA	Zweng et al. (2018)
MLD	WOA	Locarnini et al. (2018), Zweng et al. (2018)
Oxygen	WOA	Garcia et al. (2018a)
pH	GLODAPv2	Olsen et al. (2016)
Nitrate	WOA	Garcia et al. (2018b)
Phosphate	WOA	Garcia et al. (2018b)
Chlorophyll	ESACCI-OC	Sathyendranath et al. (2019)
IntPP	Eppley-VGPM-MODIS	Behrenfeld (1997)
AEU	TAOS	Foltz et al. (2019)

Note. ERA-Interim, European Center for Medium-Range Weather Forecasts atmospheric reanalysis; *WOA,* World Ocean Atlas; *GLODAP,* Global Ocean Data Analysis Project; *ESACCI-OC,* European Space Agency Climate Change Initiative - Ocean Color; *Eppley-VGPM-MODIS,* The Eppley variation of the Vertically Generalized Production Model for the Moderate Resolution Imaging Spectroradiometer; *TAOS,* Tropical Atlantic Observing System.

Each analysis includes the time evolution of the average value in the AIMPA over the whole duration of the CMIP6 simulations (1850–2100), showing both individual model means and the MMM. The recent past (2000–2010) and mid-century future (2040–2050) MMM monthly climatology are also shown. Where possible, the recent past and mid-century future MMM depth profiles are included, and their anomalies are shown separately. The spatial distribution and projected change in the wider tropical Atlantic region are shown for the recent past and the mid-century future.

Unless otherwise specified, we used the surface values in the time series, climatology and surface map analyses. The average time series, monthly climatology and vertical profile for the AIMPA are calculated using model outputs from a square region centered on Ascension Island. As shown in Figure 1, the square study region was slightly larger than the circular AIMPA. Given that CMIP6 model resolution is typically 1° by 1°, the small difference in area between the square study region and the circular AIMPA was unlikely to affect the results. The AIMPA region represented approximately 79% of the extent of the study area. The model data was used without de-drifting against pre-industrial control simulations. When showing the change between two simulated time periods, we calculated the mean of the anomalies, not the anomaly of the means. In effect, the anomaly between the two time periods was calculated first for each individual ensemble member, then the single model mean of the anomalies was calculated, then the MMM. This ensured that the differences were not biased by the historical mean and the projection mean containing a different selection of models.

While comparisons of the final years of the SSP projection time range are often made against the pre-industrial period or the recent past (e.g., Bruno et al., 2018; Garzke et al., 2017; Lotze et al., 2019; du Pontavice et al., 2020; Weijer et al., 2020), in this work we instead focused on projections of the mid-century (2040–2050). This time period was selected because it would be more relevant on policy timescales for the Ascension Island Government, who originally commissioned the analysis. This meant that the four projection scenarios would not diverge as much as if we had focused on the 2090–2100 period.

Observation-based data products were used to validate the analysis and are listed in Table 3. The annual mean of the data in the AIMPA region was included when the observational data was available as a multi-year time series, in Figures 3 and 10–12. When observational data was only available as a climatological data set, the minimum and maximum values of the data within the AIMPA region and the time period were shown as transparent rectangle with black edges, as in Figures 4–9.

2.3. Atlantic Equatorial Undercurrent Analysis

The properties of the AEU were analyzed by focusing on the state and the trend in the annual average flow, the monthly climatology, and the depth profile. The mean annual AEU flow was estimated from each ensemble member by calculating the annual mean east-west zonal velocity values along a transect at longitude 23° West, between 3° South and 3° North as shown in Figure 1, from the surface to 400 m depth. This transect encompassed the whole AEU extension and coincided with the location of the Subsurface Acoustic Doppler Current Profiler moorings, which are part of the Prediction and Research Moored Array in the Tropical Atlantic (PIRATA) mooring array (Bourlès et al., 2019; Johns et al., 2014, 2021), and the wider Tropical Atlantic Observing System (Foltz et al., 2019). By focusing on this region, we could compare model data against recent observational estimates of the AEU (Brandt et al., 2021).

The annual mean AEU flow values were obtained by taking the area-weighted sum of only the positive (west to east) velocity values in the transect area. To generate the monthly climatology, the monthly mean AEU flow values for the recent past (2000–2010) and mid-century future (2040–2050) periods were extracted from the data sets and averaged over each month. The depth velocity profiles for recent past and future periods were derived from annually averaged velocity data as the average of the two grid cells closest to the equator, which represent the location of maximal velocity. As elsewhere, the "one model — one vote" weighting scheme was applied for the MMM.

2.4. Ecosystem Services Assessment

In the ecosystem services assessment, we focused on two key habitats: the shallow sub-tidal (<30 m) and the pelagic zone (>30 m depth). Some mobile species transit between the two habitats and contribute to the ecosystem services in both zones. Due to the limited evidence of ecosystem services and climate change impacts in deep-water habitats around the AIMPA, deep-water habitats were not assessed. We identified the five most relevant ecosystem services in the region. These services were chosen on the basis of their importance to the people living on Ascension Island or visiting the AIMPA, their role in climate services, and their ecological significance. Then, a short literature review was undertaken for each habitat, which was supplemented with the expert judgment of two ecosystem service experts (SG & SB) to determine the contribution level of each ecosystem service. Three levels of contribution were used in the analysis: *minimal*, *moderate* or *significant*. Ecosystem services contributions were considered *minimal* if that service's contribution was evidenced as small compared to other habitats globally, *moderate* if locally important, and *significant* if regionally or internationally important.

Once the contribution of each ecosystem service was defined for the historical period, we then estimated how the projected change from SSP1-2.6 and SSP5-8.5 were likely to impact the ecosystem services in the future. The MMM SSP1-2.6 and SSP5-8.5 projections in the years 2090–2100 were used as the minimal and maximal boundary conditions, respectively. The 2100 horizon was used here instead of 2040–2050 as the aim was to showcase direction of travel, and the 2040–2050 period would be too soon to sufficiently differentiate the projections in this region. The future trends were graded into one of four levels: a significant reduction in ecosystem service provision, a reduction in ecosystem service provision, ecosystem services remain at a level similar to today or uncertain direction of change.

2.5. Hardware and Software Tools

The CMIP6 analyses were performed using the ESM Evaluation Toolkit, ESMValTool (Righi et al., 2020). ESMValTool is a modular python-based software toolkit that was built to facilitate the evaluation and inter-comparison of CMIP data sets. ESMValTool includes several flexible tools which can quickly standardize, extract specific regions or time periods, extract or interpolate specific depth levels, interpolate data to a new grid, and apply other statistical operators. In this analysis, we used ESMValTool to extract the AIMPA study region, extract the surface layer, extract a transect, take an area-weighted average, interpolate to a common grid, and create annual, decadal or climatological means. More details on how to access this software are available in the Open Research section, Section 6, below, and in de Mora (2023). This analysis was performed on the Center for Environmental Data Analysis's (CEDA) JASMIN computing system.

Figure 2. Summary of differences between the recent past historical period and the mid-century projected period for key metrics of the marine circulation and biogeochemistry in the Ascension Island Marine Protected Area (AIMPA). The color represents the scenario, where SSP1-2.6, SSP2-4.5, SSP3-7.0 and SSP5-8.5 are in light blue, orange, red and maroon, respectively. The y-axis shows the anomaly between the mid-century projection (2040–2050) and the recent past (2000–2010). The multi-model mean is shown as a thin horizontal line. The vertical lines represents the 5th to 95th percentile range of the single-model mean anomalies. A map of the AIMPA, the study region and the global location is shown in the bottom right of the figure.

3. Results

A summary of the results of the CMIP6 projections is shown in Figure 2. For each field, this figure shows the anomaly between the mid-century future (2040–2050) and the recent past (2000–2010). Each pane represents a different field and the colors represent the different future scenarios. In each pane, the horizontal bars shows the MMM anomalies, and the vertical line represents the 5th to 95th percentile range of the ensemble. When the 5th–95th percentile range for the anomaly overlaps with zero, there is no unanimous agreement between models in the

direction of change by 2040–2050. This figure allows a quick interpretation of the key results, whether the CMIP6 ensemble agree or diverge and includes a map of the wider Equatorial Atlantic region. Unless otherwise stated, when describing changes in the projections in this section, we compared the MMM of the mid-century future (2040–2050) against the recent past (2000–2010).

Figure 2 shows that in all models and all scenarios, the AIMPA becomes warmer, more acidic and with a lower surface phosphate concentration. Relative to the recent past (2000–2010), the multi-model means of the mid-century (2040–2050) project that the AIMPA will become warmer (+0.9 to +1.2°C), more saline (+0.01 to +0.10), with a shallower MLD (−1.3 to −0.8 m), a weaker AEU (−1.5 to −0.4 Sv), more acidic (−0.10 to −0.07), with lower surface nutrient concentrations (−0.023 to −0.0141 mmol N m^{-3} and −0.013 to −0.009 mmol P m^{-3}), lower chlorophyll concentration (−6 to −3 µg m^{-3}) and less primary production (−0.31 to −0.20 mol m^{-2} yr^{-1}). In all fields and scenarios, the MMM are in unanimous agreement on the direction of travel. All individual models agree on the future direction of travel for temperature, pH, and phosphate concentration, while the other fields show a wider spread in behavior between models and overlap with zero. In most cases, these changes are more extreme in the scenarios with higher greenhouse gases emissions and more significant climate change, except for salinity, oxygen concentration at 500 m, and nitrate and chlorophyll concentrations.

The MMM for the period 2000–2010 and 2040–2050 and the standard deviation of the ensemble of single model-means is shown in Table 4. The standard deviation was calculated as a measure of the spread of the single model means. Note that the anomalies shown in Figure 2 may not match the differences between two columns of Table 4. This is because Figure 2 shows the mean of the anomalies and the 5th-95th, but Table 4 shows the MMM and the standard deviations.

The full results of each individual CMIP6 Multimodel Analysis (CMA) are shown below, followed by the AEU then the ecosystem services analyses. Figures 3–11 all have similar composition. In these figures, pane a shows the time development of the data in the historical period (dark blue) and multiple future scenarios (light blue, yellow, red, maroon). The individual models are represented as semi-transparent lines or bands representing either only one value or the range of annual means over all contributing ensemble members. Observational data is shown as a black line or a black box in pane a. The gray and pink vertical bars indicate the recent past (2000–2010) and mid-century future (2040–2050) periods. Pane b shows the monthly climatology calculated from the two time periods. The depth profile appears in pane c and the depth profile anomaly between the mid-century future and recent past is shown in pane d, except for the 2D fields, MLD and IntPP in Figures 5 and 11. In both panes c and d of Figures 3, 4, and 6–9, the profile and profile difference panes are shown on two different z-axes scales, separated at 1,000 m by a dashed line. For the chlorophyll concentration in Figure 10, the depth profile is limited to 500 m depth with a separation at 300 m. Finally, panes e–j show maps of the data in the historical period, the observational data set, and the difference between the four mid-century future scenarios and the recent past.

3.1. Temperature

Figure 3 shows the results of the CMIP6 Multimodel Analysis (CMA) for the AIMPA temperature. In pane a, the MMM and most of the individual models overestimate the temperature relative to recent historical ERA-Interim reanalysis data (Dee et al., 2011). This bias is approximately 1°C for the MMM. In the historical period, individual models have interannual variability similar to the ERA-Interim, but the MMM has a much smoother year-to-year behavior and only shows shifts due to historic volcanic eruptions in the CMIP6 forcing data, notably Krakatoa (1883), Mt Agung (1963) and Pinatubo (1991) (Marshall et al., 2022). In the 21st century, there is a clear warming signal in the region in all projections for all models. Between the years 2000 and 2040, the MMM surface temperature rises similarly in all scenarios, but the MMMs diverge before the end of the mid-century analysis period in 2050. The decadal mean rises from 26.9°C in the recent past to 27.7°C (SSP1-2.6) or 28.0°C (SSP5-8.5) in the mid-century future. This divergence becomes even more significant toward the end of the century: The SST is projected to increase by 1.2°C in the SSP1-2.6 scenario MMM, and by 3.6°C in the SSP5-8.5 MMM by the year 2100 relative to the recent past (2000–2010).

In Figure 3b, a comparison of the historical and observational climatologies highlight that the models annual maximum occurs in March, which is earlier than the observed annual maximum in April. The bias between historical MMM and observation climatology is largest between November and April, and is very small in June and July. In the future, the warming is spread evenly over the year and the overall shape of the climatology does not change. In the mid-century future, all scenarios have a similar warming of approximately 0.8°C.
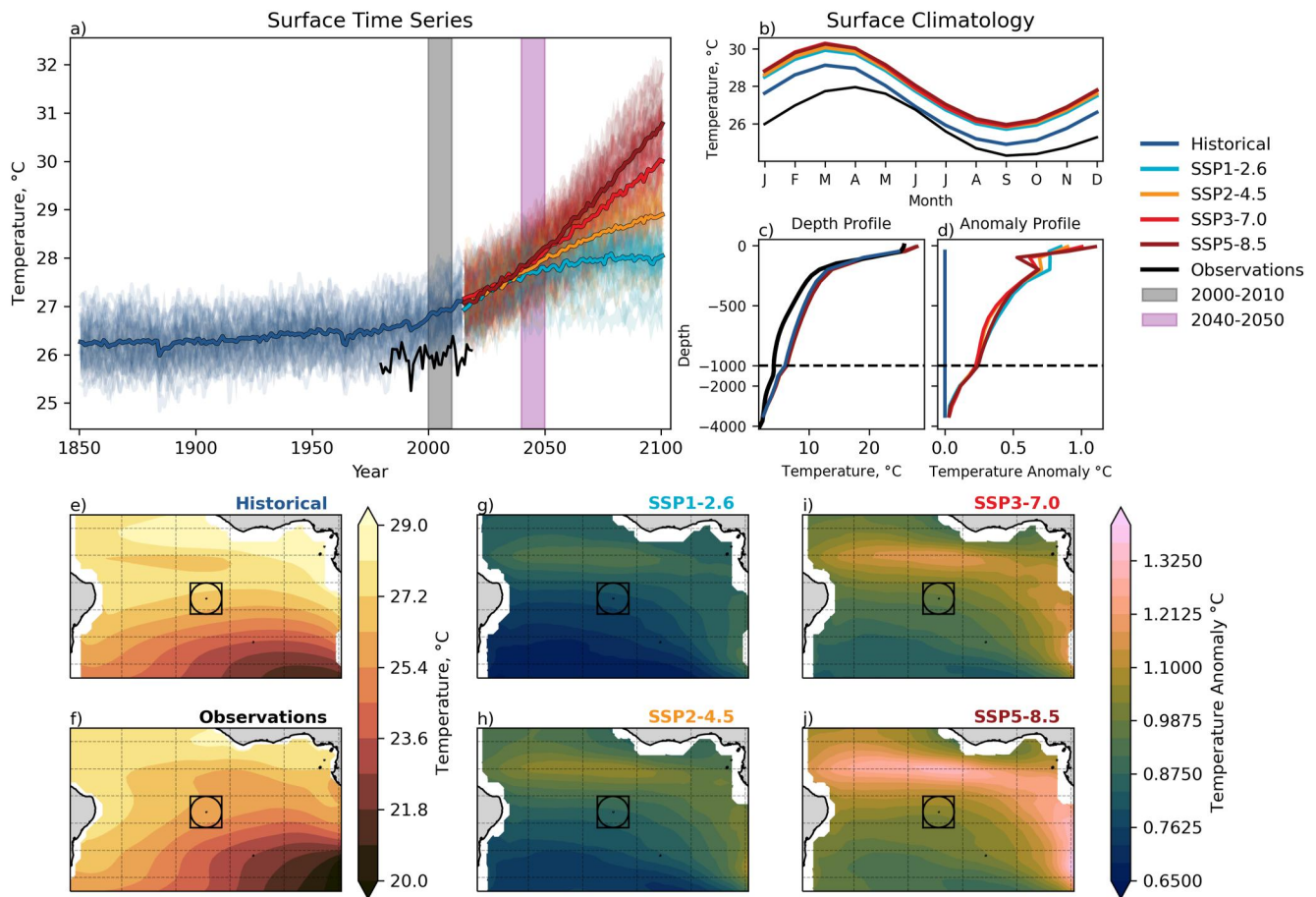
Figure 3. Coupled Model Intercomparision Project Multimodel Analysis for the Ascension Island Marine Protected Area temperature: (a) sea surface temperature (SST) time series, (b) SST monthly climatology, (c) depth profile, (d) depth profile anomaly, (e–f) maps of the historical period and the observational data set, (g–j) maps of the anomaly of the future scenarios against the historical multi-model mean. In panels (a, b), the ERA-interim reanalysis data is shown as a black line, and the WOA 2018 data is shown in panels (c, e).

As was the case for surface data, the historical MMM profile overestimates the observational data from WOA 2018 (Locarnini et al., 2018) over much of the water column in pane c. The profile and profile difference plots in panes c and d show that the projected warming occurs throughout most of the water column, with greater warming in the surface and almost no warming at the sea floor. As elsewhere, there is not a discernible divergence between MMMs for these scenarios in the mid-century future. There is an unusual feature in the subsurface around 200 m where SSP5-8.5 has less warming that SSP1-2.6, which likely indicates a substantial change in the mixing behavior and stratification at this depth.

In Figures 3e and 3f, the historical period and the WOA 2018 observation data (Locarnini et al., 2018) show very similar spatial temperature distributions in the wider equatorial and southern Atlantic region. In the mid-century future, panes g–j, the surface map panes show that the SST rises everywhere in the wider region, with the largest rise in the equatorial region. The warming in panes g–j scales with the severity of the forcing scenario, with SSP5-8.5 in pane j showing the largest change relative to the historical period.

3.2. Salinity

Figure 4 shows the CMA for salinity in the AIMPA region. In pane a, the MMM and several individual models underestimate the WOA 2018 historical surface salinity (Zweng et al., 2018) inside the AIMPA. In the future, the annual MMM salinity shows a small and gradual rise in all scenarios by the second half of the century. In the years 2040–2050, the four future scenarios show either no change or a small divergence from the historical value of 35.7 PSU, ranging from 35.7 PSU to 35.8 PSU in the mid-century future period. The SSP1-2.6 scenario has a brief
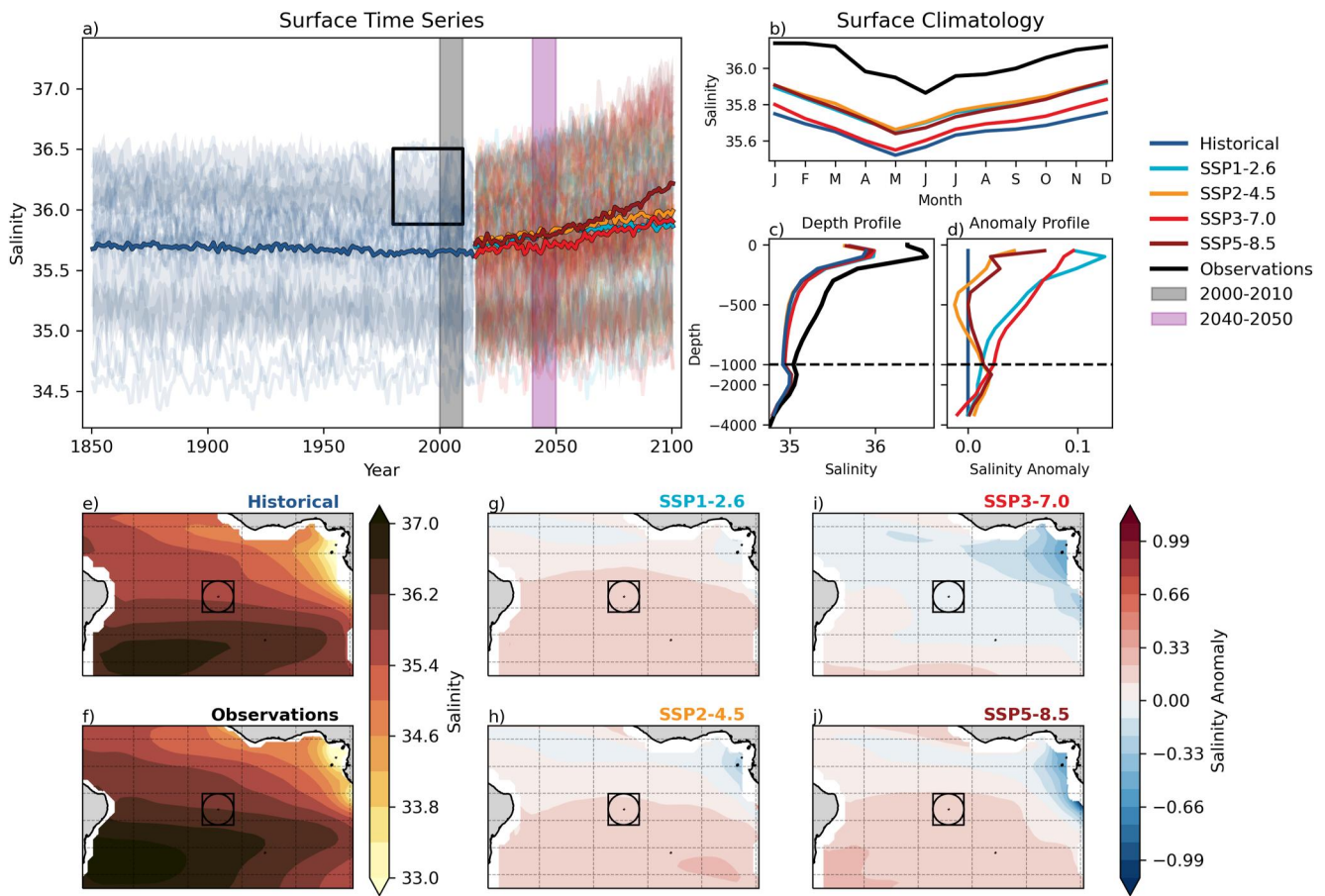
Figure 4. Coupled Model Intercomparision Project Multimodel Analysis for the Ascension Island Marine Protected Area salinity: (a) surface salinity time series, (b) monthly climatology, (c) depth profile, (d) depth profile anomaly, (e) historical period multi-model mean (MMM), (f) observational data set from WOA 2018, (g–j) maps of the anomaly of the future scenarios against the historical MMM.

period with the highest surface salinity over the years 2030–2060, but is never more than 0.06 PSU higher than the other scenarios. There are more significant differences between scenarios by the end of the century. The SSP5-8.5 MMM shows a rise in salinity around 0.5 PSU while the other three MMMs only rise around 0.2 PSU in 2100 relative to the historical period. There is a discontinuity in the ensemble mean between the historical and the future scenarios in the years 2014 and 2015. This is because the historical MMM comprises all models but only a subset of models contributed to each of the future MMMs.

In the salinity climatology, Figure 4b, the historical MMM underestimates the surface salinity over the entire year. The MMM approximately captures the overall observational seasonality but the annual minimum occurs 1 month earlier than in the observations. The SSP1-2.6, SSP2-4.5 and SSP5-8.5 projections show a similar change in climatological behavior relative to the recent past. The SSP3-7.0 projection in 2040–2050 and the historical period in 2000–2010 have similar salinity MMMs (35.7 PSU) and the other scenarios are slightly higher (35.8 PSU). While the SSP3-7.0 projection has the lowest number of contributing models, as shown in Table 1, the multi-model standard deviation for the historical and SSP3-7.0 are both 0.5 PSU, which is much larger than the range between scenarios, 0.1 PSU from Table 4.

In the depth profile, Figure 4c, the historical MMM underestimates the observational WOA2018 salinity at the surface, but overestimates the observed salinity below that point. In the future projections, the largest differences between MMMs occur above a depth of 300 m but are less than 0.1 PSU. As shown in pane Figure 4a, the SSP1-2.6 scenario MMM has the highest salinity during the years 2030–2060, but is never further than 0.06 PSU from the other scenarios through the water column.
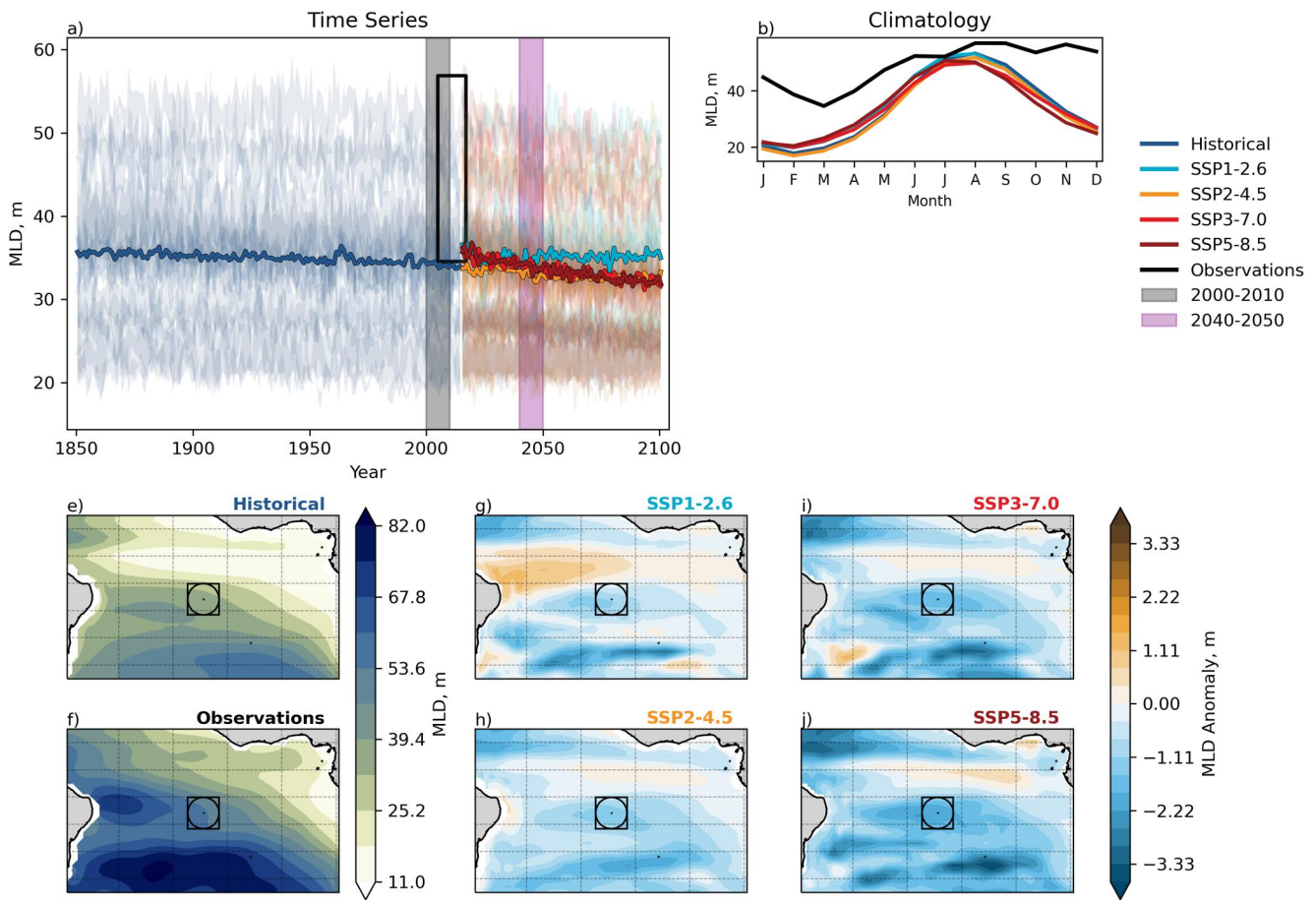
Figure 5. The CMIP6 Multimodel Analysis for mixed layer depth (MLD): (a) MLD time series, (b) monthly climatology, (e) historical period multi-model mean (MMM), (f) observational data set from WOA 2018, (g–j) maps of the anomaly of the future scenarios against the historical MMM.

In the wider region, Figures 4 and 4e–4j, all scenarios project a decline in salinity in the Gulf of Guinea, with the SSP5-8.5 scenario seeing the most freshening. This freshening plume does not reach the AIMPA in any scenario.

3.3. Mixed Layer Depth

Figure 5 shows the CMA for the MLD. This uses the CMIP6 *mlotst* field: the MLD calculated instantaneously on the model time step with a density criterion of $0.125 \, \mathrm{kg \, m^{-3}}$ (Griffies et al., 2016). The observational MLD data is from the World Ocean Atlas, WOA (Locarnini et al., 2018; Zweng et al., 2018), and is the depth for which the potential density has increased by $0.125 \, \mathrm{kg \, m^{-3}}$ relative to the 10 m reference depth. There are many MLD calculation methodologies (Cabanes et al., 2013; de Boyer Montegut et al., 2004; Griffies et al., 2016; Locarnini et al., 2018; Zweng et al., 2018), we ensured that the model and observational data can be compared by using the density method with the same threshold criterion.

In Figure 5a, the modeled time series and the observational range overlap, with the MMM approximately equal to the lowest values seen of the observations. The AIMPAs MLD in recent past MMM is 34.1 m, and the mid-century future MLD is projected to become slightly deeper in the SSP1-2.6 scenario (35 m), shallower in the SSP2-4.5 scenario (33 m) and remain approximately the same in the SSP3-7.0 (34 m) and SSP5-8.5 (33.9 m) scenarios. At the end of the century, the MLD is projected to remains constant in the SSP1-2.6 scenario but to become shallower in the other three scenarios.

In the MLD climatology, Figure 5b, the models underestimate the observed values throughout the year, and the MMM minimum occurs in February while the observational annual minimum occurs in March. The MMM also show a significant end of year shallowing in September–December that is not present in the observational data. In
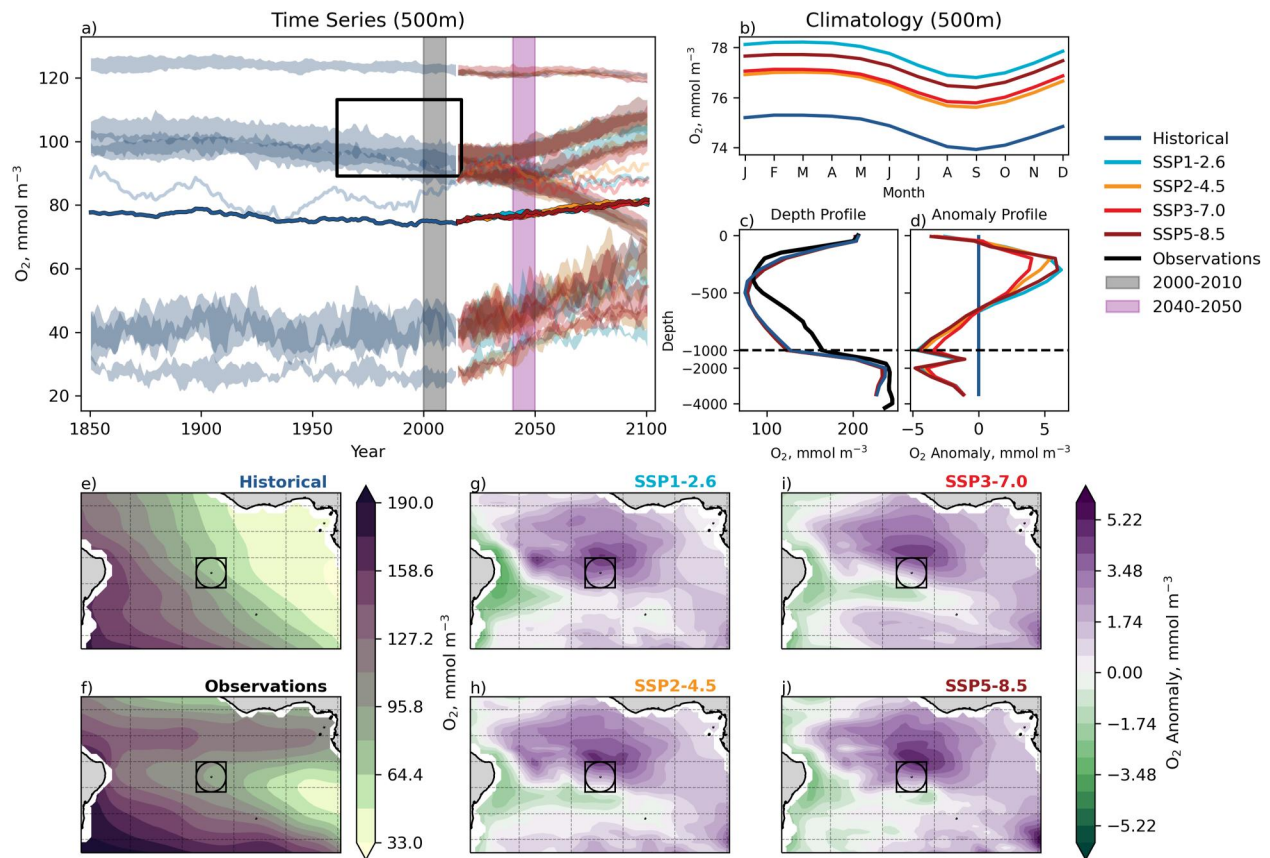
Figure 6. The dissolved oxygen concentration at 500 m CMA: (a) time series, (b) monthly climatology, (c) depth profile, (d) depth profile anomaly, (e) historical period multi-model mean (MMM), (f) observational data set from WOA 2018 (Garcia et al., 2018a), (g–j) maps of the anomaly of the future scenarios against the historical MMM.

the SSP5-8.5 projection, the deepest MLD occurs in July, 1 month earlier than the historical period's deepest MLD. The other projections show changes to the MLD range but do not show changes in the timing of the minimum or maximum MLD.

In the spatial distributions in Figures 5e and 5f, the historical MMM reproduces the overall spatial distribution of the WOA data, but has a shallow bias over most of the region. This bias is particularly strong to the south and to the west of the AIMPA, where the MMM MLD is up to 40 m shallower than in the observational data. The AIMPA sits inside a band of shallowing MLD in all future scenarios. This shallowing band ranges from 1 to 3 m inside the AIMPA and extends across most of the Atlantic Ocean. A MLD deepening of between 0.5 and 1.5 m is seen along the path of the Equatorial Current in all four projections. The impact of the changing climate on MLD scales with the severity of the climate forcing in this region for this ensemble of models, with SSP5-8.5 showing the largest changes.

3.4. Dissolved Oxygen Concentration at 500 m

The oxygen concentration at 500 m CMA is shown in Figure 6. The 500 m depth was selected because the modeled water column minimum oxygen concentration occurs at this depth. In the time series in pane a, there is little agreement between models in either the historical range or the future direction of travel. In the future time series, some models project a strong decline, others project an increase, while some project no significant change in either direction. Each of the MMMs project a small rise in oxygen concentration at 500 m from 75 mmol m^{-3} in the recent past to 76 mmol m^{-3} in SSP2-4.5 and SSP3-7.0, 77 mmol m^{-3} in SSP5-8.5 and 78 mmol m^{-3} in SSP1-2.6 in the mid-century future. This inter-model uncertainty is a result of oxygen concentrations being strongly influenced by simultaneous changes in solubility, circulation, and mixing, and biological sources and sinks (Kwiatkowski et al., 2020). The oxygen at depth is particularly sensitive to how the hydrodynamics of the area are

represented, particularly stratification and circulation (Schmidtko et al., 2017). Furthermore, the representation of the hydrodynamics in CMIP6 models is sensitive to parameter choice, which varies between models (Herrera et al., 2022).

Figure 6b shows that all scenarios project a small rise in the MMM climatological oxygen concentration at 500 m relative to the recent past and this rise is spread evenly throughout the year. The SSP1-2.6 scenario has a slightly larger rise in climatological oxygen concentration than the other scenarios. This is likely due to the small dip in the MMM oxygen concentration at 500 m in the years 2035–2045 in the three other scenarios, which can be seen in Figure 6a. This dip is not a permanent feature and the four scenarios MMMs do not diverge before the end of the 21st century. The observational data is not shown in pane b because the offset against observations is significantly larger than the difference between scenarios. In either case, there are no clear differences between scenarios in the MMM climatological oxygen concentration and the differences between scenarios are significantly less than the differences between individual models in Figure 6a.

In the depth profile in Figure 6c, the MMM reproduces the overall observational patterns of the observations in the AIMPA, but includes a large bias between 300 and 1,000 m depth. The MMM captures the observational surface values but the modeled minimum oxygen concentration occurs shallower than in observations. The MMM also slightly underestimates the oxygen below 2,000 m. The differences between the recent past and the mid-century projection are more apparent in pane d. All scenario MMMs project de-oxygenation above 100 m and below 700 m, and a rise in oxygenation between 100 and 700 m where the largest rises in oxygen coincide with the observed minimum oxygen concentration. This is in agreement with Kwiatkowski et al. (2020), who showed that the equatorial Atlantic is one of the few regions in the global ocean where the subsurface (100–600 m depth) dissolved oxygen concentration is projected to rise in the long term.

In the spatial distribution of WOA 2018 oxygen at 500 m in pane f, a region with low oxygen concentration extends from the Angola Basin to the AIMPA, and the equatorial region, the western South Atlantic and the southern Atlantic have higher oxygen concentrations than the AIMPA. However, the MMM shows a gradual rise in oxygen concentration at 500 m from east to west. The low oxygen concentration at 500 m region is not captured in the recent past MMM or any of the individual model distributions (not shown). In the future projections, the oxygen concentration at 500 m in the equatorial Atlantic is projected to rise in all scenarios, mirroring the findings of Kwiatkowski et al. (2020). The oxygen concentration at 500 m is projected to either decline or remain constant in the southern Atlantic, and decline along the western edge of the South Atlantic. While the differences between individual projections and between the historical simulation and future projections are small, they result from a large inter-model spread seen in Figure 6a and hence these projections can be considered to have a large uncertainty.

3.5. pH

Figure 7 shows the CMA for pH in the AIMPA region. In the surface pH time series in Figure 7a, there is a very tight agreement between the individual models with a spread of less than 0.1 at all times. In addition, the models are in agreement with the GLODAPv2 observational data (Olsen et al., 2016). Similarly, there is a very tight grouping of model ensembles within each future projection. Compared to the recent pasts pH MMM of 8.05, the mid-century future pH is projected to range from 7.98 in the SSP1-2.6 scenario to 7.95 in SSP5-8.5. This is expected as the surface pH in open ocean waters is strongly anti-correlated to the atmospheric carbon dioxide (CO_2) concentration (Whitfield, 1975) and the atmospheric CO_2 concentration is a prescribed variable in each scenario and thus is identical between models. In all cases, the change in pH between the recent past and the mid-century scales with the scenarios emissions. While the others scenarios project a continual acidification, the SSP1-2.6 scenario projects the start of the recovery in the surface pH by the end of the 21st century. Although it is shown in panes d, and g–j, the difference between two pH values does not scale linearly due to pH's logarithmic scale. For instance, a decrease in pH of −0.5 means the water has become 3.2× more acidic, while a decrease in pH change of −1.0 means the water has become 10× more acidic. However, pH anomaly is nevertheless shown here as it is a widely accepted metric for acidification.

In Figure 7b, the pH climatology of the recent past is lower than the observational range for the months January–May, but they overlap across June–December. This is likely because the observations include data from an earlier time range (1973–2013) than the recent past (2000–2010), so the observational climatology is likely be weighted toward years with lower atmospheric CO_2 concentration and higher surface pH. In the future projections, the
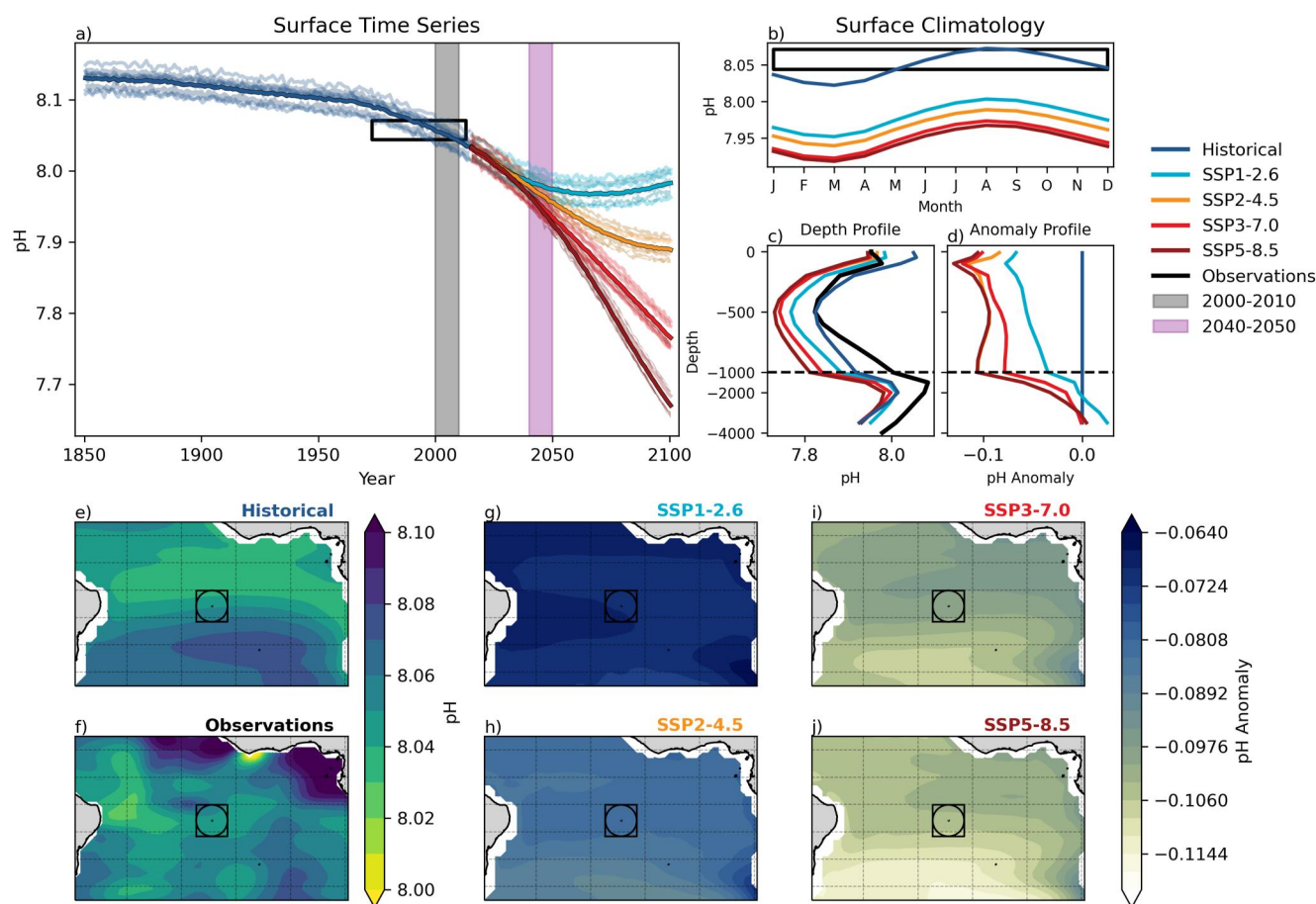
Figure 7. The surface pH CMA: (a) time series, (b) monthly climatology, (c) depth profile, (d) depth profile anomaly, (e) historical period multi-model mean (MMM), (f) observational data set from GLODAPv2 (Olsen et al., 2016), (g–j) maps of the anomaly of the future scenarios against the historical MMM.

higher emission scenarios lead to a lower surface pH than the lower emission scenarios throughout the climatology. The scenarios SSP3-7.0 and SSP5-8.5 do not yet diverge by the mid-century. For all projections of the mid-century, the climatological maximum pH will be below the annual minimum of the recent past.

The pH depth profile in Figure 7c shows that while the historical MMM and GLODAPv2 observational data (Olsen et al., 2016) agree at the surface, they diverge between 200 and 700 m where the historical MMM is higher than the observed pH. However, there is a little divergence between projections over the water column. At depth, pH becomes decoupled from the atmospheric CO_2 forcing and more influenced by local hydrodynamics, similarly to the oxygen in Figure 6. The profile difference in Figure 7d shows that the pH change in the four scenarios scales with the severity of the climate forcing from the surface downwards.

Figures 7e and f show the MMM recent past historical pH and the GLODAPv2 observational data respectively. The observational data has significantly higher pH in the Gulf of Guinea and the Sierra Leone Basin regions, while the historical MMM is much more homogeneous. The mid-century projection anomaly in panes g–j are also homogeneous, with large regions of the surface showing little variability. This is expected as the surface pH is linked to the spatially homogeneous atmospheric CO_2 forcing, and taking the mean of several models will add further homogeneity.

3.6. Nitrate Concentration

Figure 8 shows the CMA for nitrate concentration. There is a significant diversity in the range of the single-model mean surface nitrate concentrations in this ensemble in Figure 8a. However, the historical MMM captures the center of the range of the WOA 2018 observational data set of surface nitrate concentration (Garcia et al., 2018b).
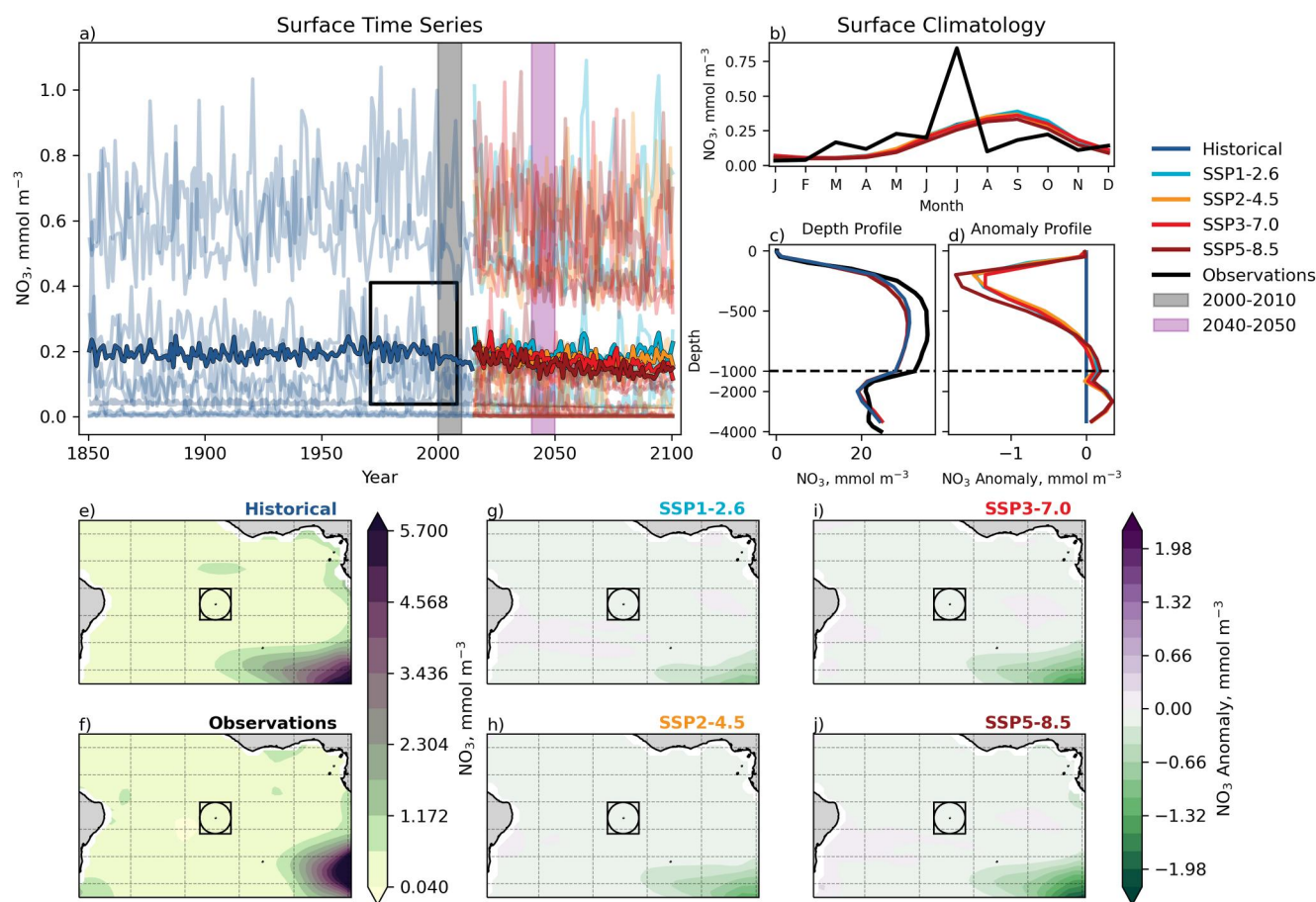
Figure 8. The dissolved nitrate concentration CMA: (a) surface time series, (b) surface monthly climatology, (c) depth profile, (d) depth profile anomaly, (e) historical period multi-model mean (MMM), (f) observational data set from WOA 2018 (Garcia et al., 2018b), (g–j) maps of the anomaly of the future scenarios against the historical MMM.

Compared to the nitrate concentration of 0.18 mmol m^{-3} in the recent past, the mid-century future nitrate concentration is projected to range from 0.15 mmol m^{-3} in SSP5-8.5 to 0.22 mmol m^{-3} in the SSP1-2.6 scenario. In the future, a very small decline in the MMM surface nitrate concentrations may be seen when comparing the start of the projected time range against the end. There is a discontinuity in Figure 8a at the year 2015 between the end of the historical period and the start of the projection which is caused by differences in the MMM ensembles. The size of the historical-future discontinuities are all significantly smaller than the difference between the historical MMM and the observational range.

In the surface nitrate concentration climatology in Figure 8b, the MMMs do not capture the mid-year peak or the August drop in surface nitrate concentration in the WOA 2018 observational data. However, the models do capture annual minimum in January–February. The MMMs have a smoother and more gradual annual cycle than the WOA data. In the mid-century future, the SSP1-2.6 scenario shows a slightly higher annual maximum in September, but otherwise the four projections do not visibly diverge from each other or from the historical climatology.

Figure 8c shows the MMMs and WOA 2018 nitrate concentration profiles. The historical MMM captures the WOA 2018 nitrate concentration depth profile over the top 300 m. The historical MMM and observations diverge below this depth, with the MMM underestimating the observations between 300 and 2,500 m. In the future, the MMMs project a decline in nitrate concentration in the top 700 m of the water column and a rise below that.

The surface nitrate concentrations in the historical MMM and the observational spatial distribution are shown in Figures 8e and 8f. The recent past MMMs captures much of the behavior of the WOA 2018 surface nitrate concentration, and they both show very low surface nitrate concentrations over much of the equatorial Atlantic,
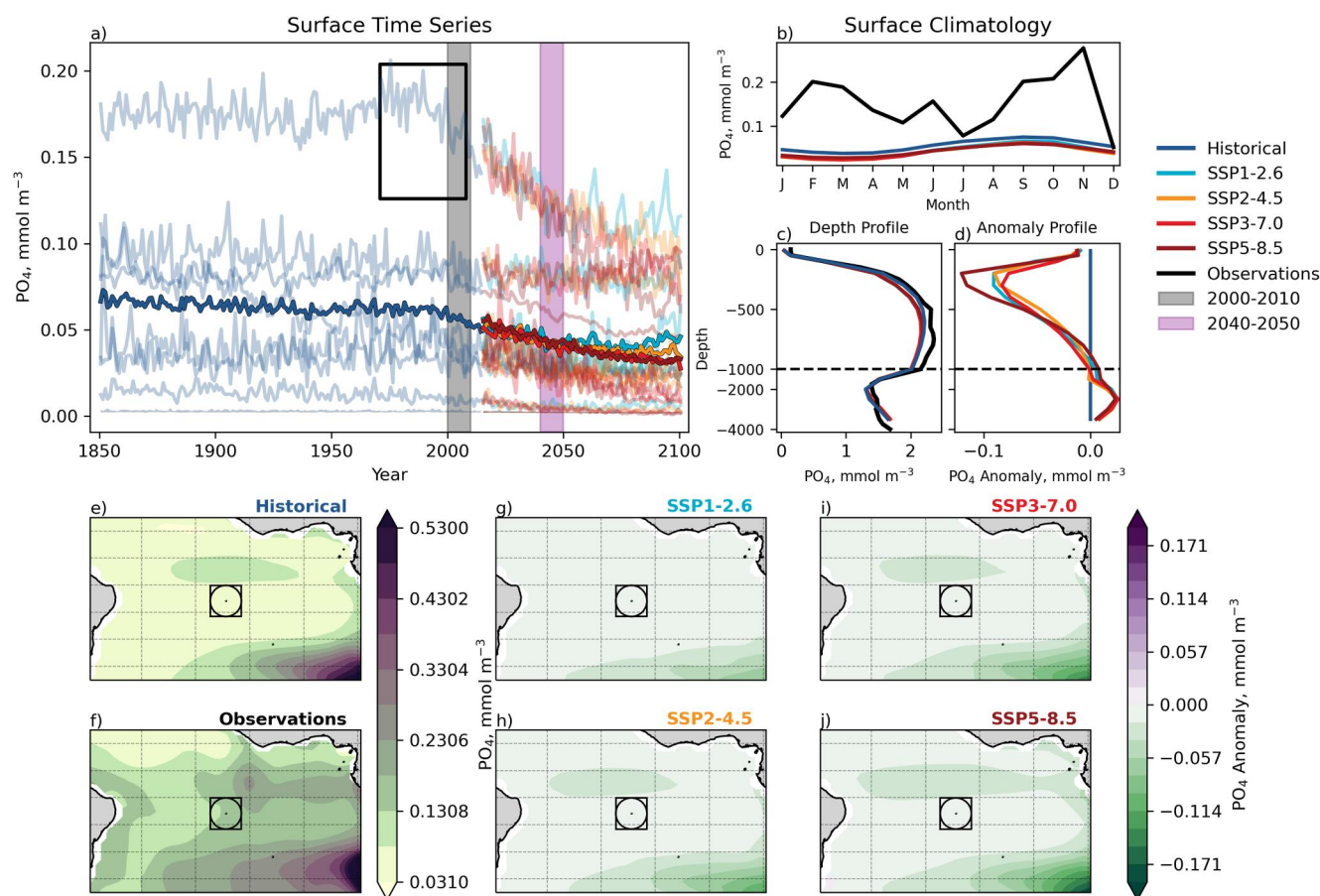
Figure 9. The dissolved phosphate concentration CMA: (a) surface time series, (b) surface monthly climatology, (c) depth profile, (d) depth profile anomaly, (e) historical period multi-model mean (MMM), (f) observational data set from WOA 2018 (Garcia et al., 2018b), (g–j) maps of the anomaly of the future scenarios against the historical MMM.

with the highest values to the southeast in the Benguela upwelling region. In the future, all four projections show similar behaviors with little change in surface nitrate concentrations around the AIMPA. The SSP5-8.5 scenario shows the largest decline in the nitrate concentrations in the Benguela upwelling region.

In all historical simulations and in the observational data, the AIMPA surface layers have low nitrate concentrations. A typical value is around 0.2 mmol m^{-3} at the surface, but the maxima in the water column is closer to 30 mmol m^{-3} at 500 m. In all projections, the surface nitrate concentration in the AIMPA will remain low in the future.

3.7. Phosphate Concentration

Figure 9 shows the CMA for phosphate concentration. There is a wide range of behaviors in the models for the mean surface phosphate concentrations time series in Figure 9a. The historical MMM significantly underestimates the WOA 2018 observational range (Garcia et al., 2018b). Only one model, CESM2, captures the observational range in the historical period. In the future, a decline in the surface phosphate concentrations is projected for most individual models and the MMMs. The MMM phosphate concentration was 0.06 µmol m^{-3} in the recent past, and this is projected to drop to 0.04 µmol m^{-3} in all four scenarios in the mid-century future period. The four projections do not diverge by the mid-century future period but they do diverge by the end of the century. The MMM surface phosphate concentration in the SSP5-8.5 has continued to decline over the period 2050–2100, while the SSP1-2.6 scenario has stabilized from 2050.

In the surface phosphate concentration climatology in Figure 9b, the historical MMM does not capture the overall shape or the range of the WOA 2018 observational data, notably the early year peak in February–March, the late

year peak in September–November or the mid-year dip in July. There is no projected change in the phenology of the surface phosphate concentration. There is no visible difference between the four scenarios in the mid-century projections, and the previously described shift of -0.02 μmol m^{-3} occurs evenly throughout the year.

In the depth profile in Figure 9c, the historical MMM captures the depth-behavior of the observed data: the surface is phosphate depleted, there is a maxima below 500 m and a local minima around 2,000 m. The historical MMM underestimates the observed phosphate concentrations between 300 and 1,500 m. In Figure 9d, the projections show decline between the surface and 1,000 m, and a slight rise below 1,000 m. The scenario SSP5-8.5 shows the largest decline in phosphate concentration in this depth range while the other three scenarios all have a slightly smaller phosphate concentration anomaly in this depth range.

The spatial distribution of the recent past MMM and the WOA 2018 surface phosphate concentration are shown in Figures 9e and and 9f. As in Figure 9a, the historical MMM underestimates the observed values inside the AIMPA, and this underestimated region extended over most of the southern Atlantic. But does show a similar spatial pattern to the observational data. There is a regional maxima in the Benguela upwelling system and a local maximum to the north of the AIMPA along the equatorial current. However, the MMM does not capture the local maximum that appears in observational data off the coast of South America. In the future, the four projections all show similar behaviors in the AIMPA surface phosphate concentration. All scenarios project a decline in the surface phosphate concentration in the Benguela upwelling region, with the largest decline in the SSP5-8.5 scenario. This is in agreement with the nitrate concentration in Figure 8, suggesting a potential slowdown of the Benguela upwelling current by the mid-century period.

The change in phosphate concentrations is small in absolute terms because the AIMPA phosphate concentrations is already very low in the recent past historical period. This is because the AIMPA is in an open ocean — low nutrient region. Nevertheless, the relative change in phosphate concentration between the two time periods is significant, with phosphate concentration projected to decline by between -0.02 and -0.01 μmol m^{-3}, which is up to a third of its historical MMM. The decline in the MMM surface phosphate concentration starts around the year 1995 in Figure 9a, before the recent-past historical period (2000–2010). This means that the MMM values shown in Table 4, Figures 2 and 9b–9d and 9g–9j miss the start of the decline. These values likely underestimate the magnitude of the overall decline relative to a pristine pre-industrial environment.

3.8. Chlorophyll

Figure 10 shows the CMA for chlorophyll concentration. The MMM timeseries in Figure 10a captures the range of the ESACCI-OC observational timeseries (Sathyendranath et al., 2019), but there is a wide diversity in the biases of individual models. Six of the eight models here project a decline in surface chlorophyll concentration while one model has no significant change (CMCC-ESM2) and one model projects a large rise (CanESM5). The MMMs of the four scenarios project declines from 116 μg m^{-3} in the recent past to between 105 and 109 μg m^{-3} in the mid-century future. Unlike other analyses, the MMM SSP5-8.5 scenario projects the smallest decline in surface chlorophyll concentration. This is likely due to a strong increase of 100 μg m^{-3} in CanESM5's surface chlorophyll concentration, which dominates the MMM, and overbalances the relatively small declines in chlorophyll concentration shown by the other models.

The climatological MMM surface chlorophyll concentration does not fully capture the observational behavior in Figure 10b: the annual peak occurs one month too late in October, and is significantly lower than the observed maxima (152 vs. 215 μg m^{-3}). The MMM also has an extended annual minimum between February and May while the annual minimum in the observations has a shorter period of low chlorophyll concentration with a minimum in March. In the mid-century future, the MMMs project that the shape of the seasonal cycle of surface chlorophyll concentration will remain intact, but the peak will be reduced, indicating either lower phytoplankton abundance or lower Chl:C ratios or both in the future.

In the depth profiles in Figures 10c and 10d, the chlorophyll concentration peaks at 100 m, and drops to close to zero at 200 m. The observational data elsewhere in Figure 10 is satellite-derived ocean color, so there is no depth component available. The depth below 500 m is very close to zero and not shown. In the anomaly in Figure 10d, the four scenarios show some small difference shallower than 200 m, but the MMMs do not diverge by the mid-century.
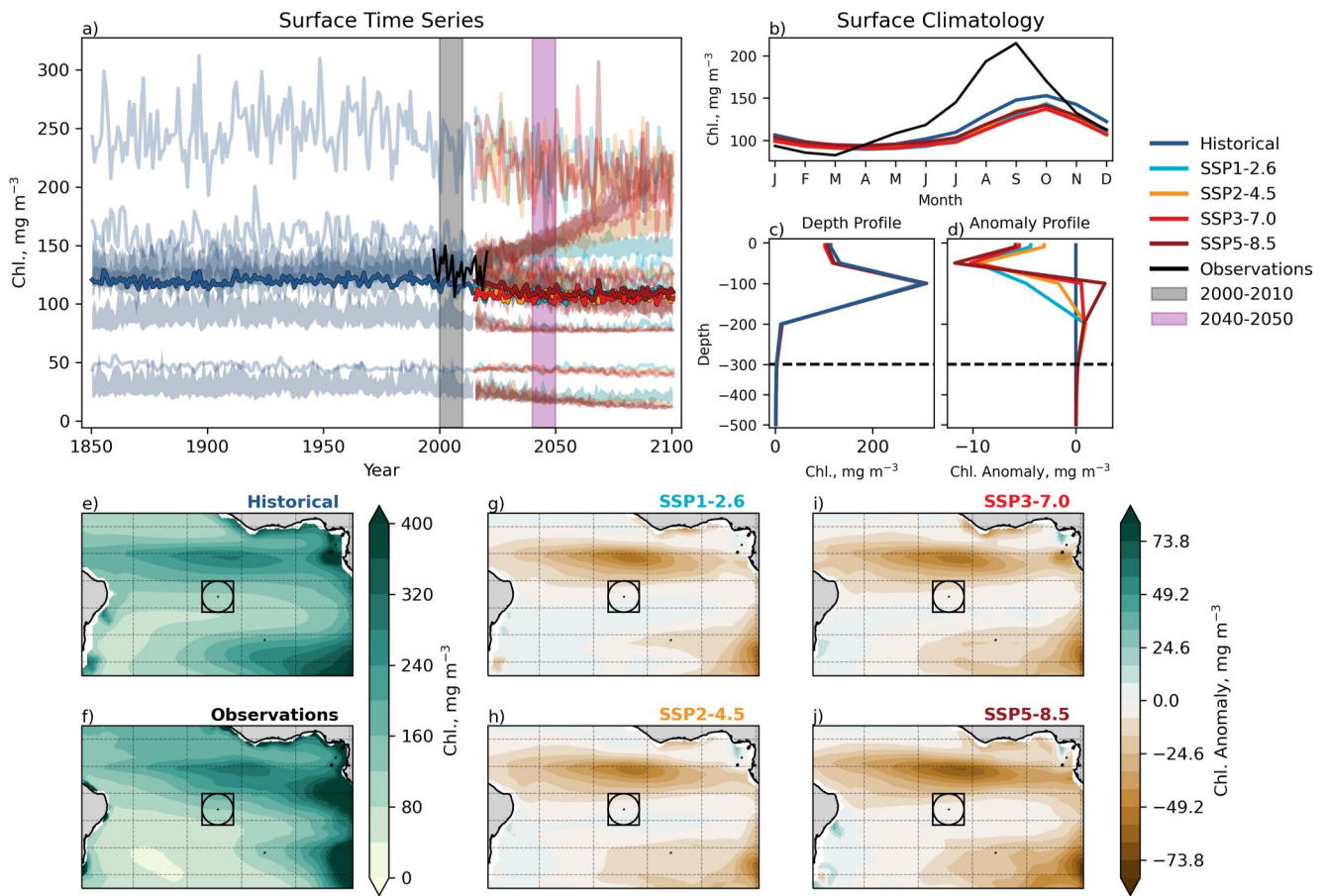
Figure 10. The chlorophyll concentration CMA: (a) surface time series, (b) surface monthly climatology, (c) depth profile, (d) depth profile anomaly, (e) historical period multi-model mean (MMM), (f) observational ESACCI-OC data set (Sathyendranath et al., 2019), (g–j) maps of the anomaly of the future scenarios against the historical MMM.

In the spatial distributions in Figures 10e–10j, the ensemble mean reproduces much of the wider patterns in historical observations in the region, especially the higher production of the equatorial Atlantic and in the Benguela upwelling region, and the lower production in the South Atlantic. In the mid-century future, all MMMs project a large decline along the equator and to the southeast of the AIMPA, but a much smaller decline within the AIMPA. In all scenarios in Figures 10g–10j, a decline in surface chlorophyll concentration is projected over almost the entire southern Atlantic region, except for few small regions in coastal waters to the west of the Atlantic and a narrow band to the south of the AIMPA.

3.9. Integrated Primary Production

Figure 11 shows the CMA for IntPP. In Figure 11a, the MMM underestimates the Eppley-VGPM-MODIS observational mean (Behrenfeld, 1997) in the recent past by approximately 2 mmol m^{-2} d^{-1}. The MMM visibly fails to capture the interannual variability in the observational data, while some of the single models show variability of similar order to the observational data. Like the chlorophyll concentration in Figure 10, some models project a decline but others models project a rise in IntPP. When combined, the declining models outbalance the rising models and the MMM projections decline to between 10.7 mol m^{-2} yr^{-1}–10.9 mol m^{-2} yr^{-1} in the mid-century future relative to the 11.4 mol m^{-2} yr^{-1} in the recent past. A decline in the MMM starts in the year 1995, which is in agreement with the decline in surface nutrient concentrations in Figures 8a and 9a.

The climatological MMMs do not fully reproduce the observational seasonal cycle in Figure 11b. The MMM annual peak is delayed by 1 month to October, and is lower (13.2 vs. 15.8 mol m^{-2} yr^{-1}). In the mid-century projections, the climatological behavior retains the same shape as the recent past between July and February,
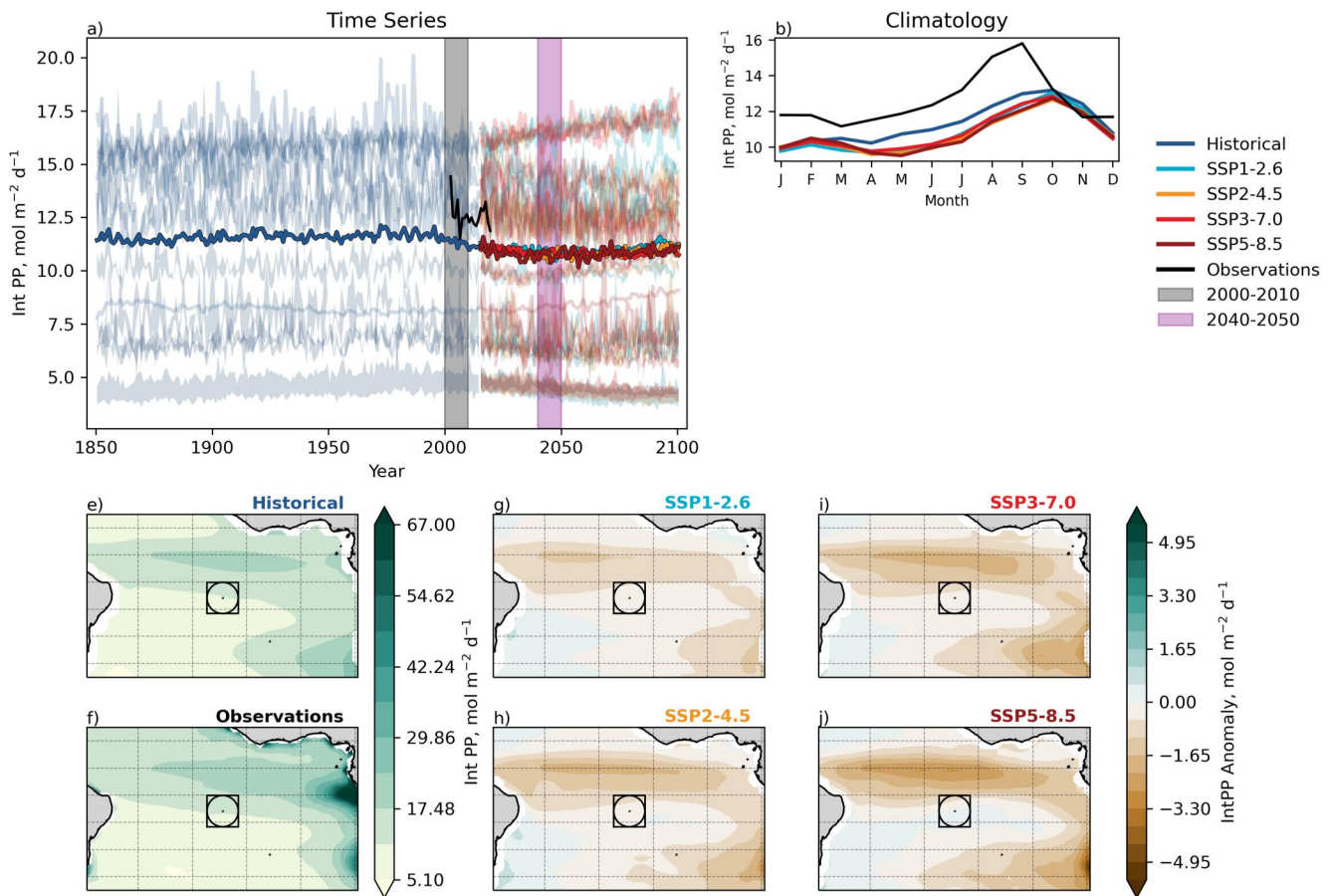
Figure 11. The Integrated Primary Production CMA: (a) surface time series, (b) surface monthly climatology, (e) historical period multi-model mean (MMM), (f) observational Eppley-VGPM-MODIS data set (Behrenfeld, 1997), (g–j) maps of the anomaly of the future scenarios against the historical MMM.

but include a more significant drop in March to July. The historical annual minimum was in January, but the annual minimum is projected to be in April or May in the mid-century. However, the MMM IntPP in January is still low and there is a small local maxima in February.

In the wider region, the MMM reproduces the spatial distribution of the observations in Figures 11e and 11f, but has a lower maxima in the Benguela upwelling region and a narrower equatorial local maxima. In the mid-century future in Figures 11g–11j, all scenarios show a decrease in the MMM IntPP over the equatorial Atlantic region, with the largest changes closer to the equator in SSP5-8.5. All scenarios project a decline in the primary production in the Benguela upwelling region, with the magnitude of the decline scaling with the strength of the climate change forcing and the largest decline in the SSP5-8.5 scenario.

3.10. Atlantic Equatorial Undercurrent Analysis

Figure 12 shows the CMA of the AEU. Figure 12a shows the time evolution of the mean annual AEU in the historical and future scenarios, compared with observational estimates for the 2005–2019 period (Brandt et al., 2021). The average value of the AEU flow during the historical period is 16.3 Sv and ranges between 12.8 and 21.5 Sv. This is within the range of values reported in the literature: between 14.0 and 18.0 Sv (Brandt et al., 2021; Hormann & Brandt, 2007). Little change can be seen in the AEU flow during the historical period, but all future scenarios project a decline in the mean annual flow. The decrease ranges from −0.3 to −0.07 Sv/decade. In SSP5-8.5, the AEU decreases by −6.1% by 2050 and by −14.2% by 2100. The rate of change is projected to be relatively constant over the coming century, except for in the SSP5-8.5 scenarios, where the strength of the AEU decreases faster in the second half of the century.
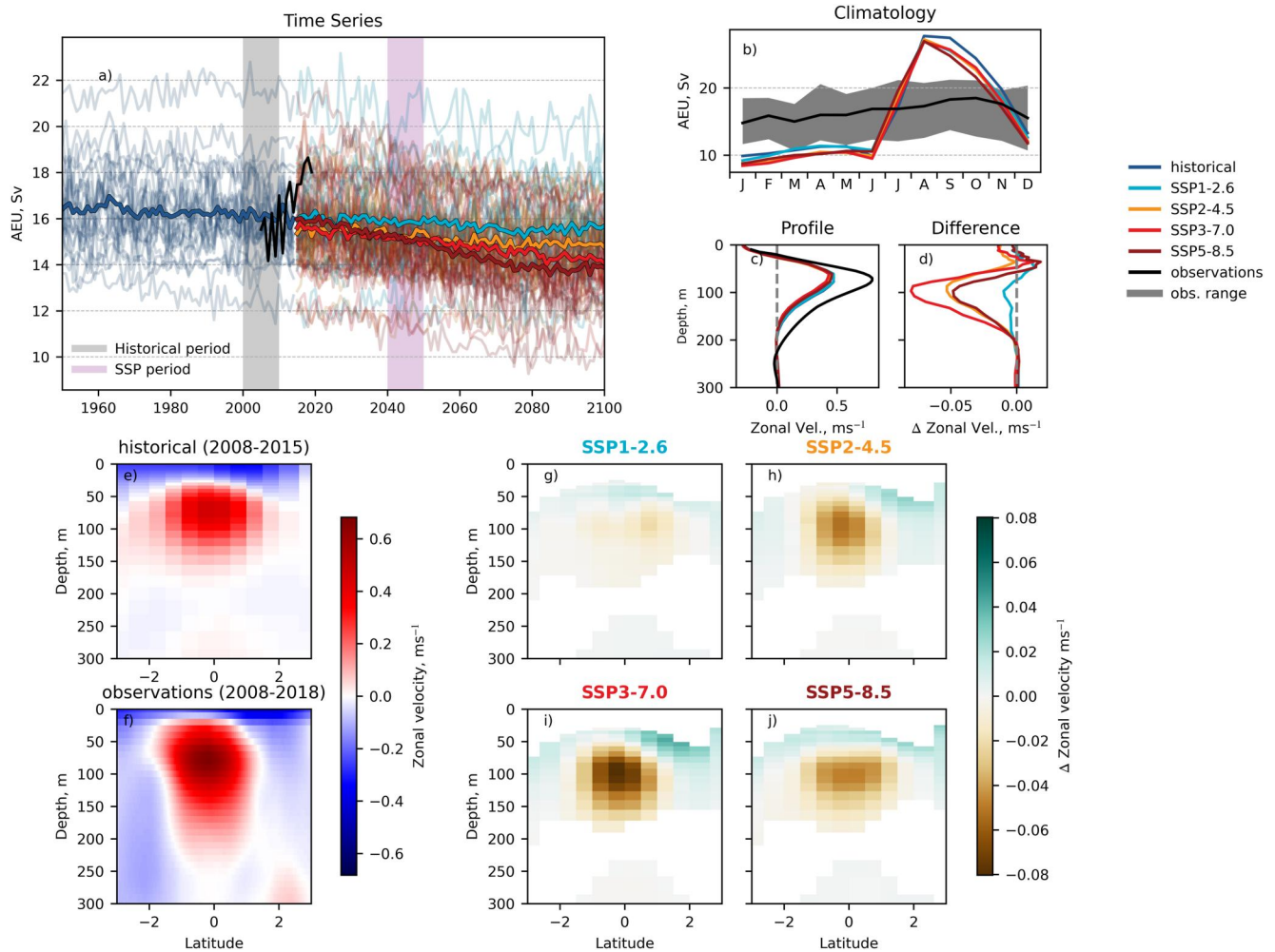
Figure 12. The Atlantic Equatorial Undercurrent CMA: (a) time series, (b) monthly climatology, (c) depth profile, (d) depth profile anomaly, (e) historical period velocity field, (f) observational velocity field (Brandt et al., 2021), (g–j) the anomaly of the future scenarios against the historical multi-model mean velocity fields.

Table 4
The Multi-Model Mean and the Standard Deviation of the Ensemble of Single Model-Means for Each Variable in the Study

Field	Historical	SSP1-2.6	SSP2-4.5	SSP3-7.0	SSP5-8.5
Years	2000–2010	2040–2050	2040–2050	2040–2050	2040–2050
Temperature, °C	26.9 ± 0.4	27.7 ± 0.4	27.8 ± 0.4	27.9 ± 0.4	28.0 ± 0.4
Salinity, PSU	35.7 ± 0.5	35.8 ± 0.5	35.8 ± 0.4	35.7 ± 0.5	35.8 ± 0.4
MLD, m	34.1 ± 8.1	35.0 ± 8.2	33.0 ± 8.0	34.0 ± 8.9	33.9 ± 8.3
Oxygen (500 m), mmol m^{-3}	75 ± 32	78 ± 28	76 ± 29	76 ± 29	77 ± 28
pH,	8.05 ± 0.01	7.98 ± 0.01	7.97 ± 0.01	7.95 ± 0.01	7.95 ± 0.01
Nitrate, mmol m^{-3}	0.18 ± 0.22	0.18 ± 0.21	0.17 ± 0.21	0.18 ± 0.21	0.15 ± 0.20
Phosphate, μmol m^{-3}	0.06 ± 0.05	0.04 ± 0.04	0.04 ± 0.04	0.04 ± 0.04	0.04 ± 0.04
Chlorophyll, μg m^{-3}	116 ± 60	106 ± 61	107 ± 63	105 ± 59	109 ± 59
IntPP, mol m^{-2} yr^{-1}	11.4 ± 3.8	10.8 ± 4.2	10.7 ± 4.1	10.9 ± 4.0	10.7 ± 3.8
AEU, Sv	16.2 ± 2.0	15.8 ± 2.0	15.2 ± 1.6	14.9 ± 1.6	14.7 ± 2.0

Long-term mooring observations show a strengthening of the AEU by 20% in the 2005–2019 period (Brandt et al., 2021). While a trend is observed over the observational period, the authors attributed it to multi-decadal natural variability of the undercurrent, not anthropogenic climate change. There is no overall strengthening trend in the historical MMM AEU in the recent past, but variability of the same order of magnitude can be seen in the single-model means. ESMs do not represent the exact phase of the climate system nor the timing of climate variability relative to historical observations, so we did not expect them to reproduce the observed strengthening.

The AEU climatology is shown in Figure 12b, along with the range of values reported by Brandt et al. (2021). The MMM shows a clear seasonal behavior with lower transport in January-June and higher transport during July–December. While observations show a similar timing of the seasonal minimum and maximum, the amplitude of the seasonal cycle is much higher in the models than in the observations.

The velocity profile at the equator is shown in Figure 12c. The recent past MMM agrees with the observational data and places the peak AEU between 50 and 200 m depth, but the MMM simulates a slower peak velocity and a shallower zero current at 150 m instead of the observed value of 200 m. In Figure 12d, a weakening of the AEU is projected in the future scenarios, mostly taking place at 80 m depth and below.

Figures 12e and 12f show the comparison between the CMIP6 average profile and the AEU velocity profile along the AEU transect reconstructed from Brandt et al. (2021) at 23° West. The location and strength of the AEU are well captured by the model average despite the recent past MMM overestimating the latitudinal extension and underestimating the depth extension of the current. This is expected given the coarse resolution of the CMIP6 models and averaging over many members smooths out peak values.

Figures 12g–12j show the anomaly between the mean AEU velocity field in the four future scenarios for the years 2040–2050 and the historical ensemble in the years 2000–2010. Negative currents flowing from east to west in the historical period were masked to highlight changes in the AEU. All projections show a weakening of the velocity field between 75 and 200 m depth. This is partially counterbalanced by an increase in velocity at shallower depths. The future scenario that shows the largest change is SSP3-7.0, where the peak velocity decreases by around 0.08 m s^{-1}. This reduction in peak velocity is partly balanced by an increase in velocity in the shallower and northern region so that the annual mean current in this scenario by 2050 is close to that projected in the higher emission scenario, SSP5-8.5, in Figure 12a. After 2050, the two scenarios diverge with the strongest weakening of AEU being projected in SSP5-8.5.

3.11. Ecosystem Services Assessment

The results of the Ecosystem service assessment are shown in Figure 13. This figure summarizes the importance of each ecosystem service for both the shallow subtidal and pelagic habitats, and shows how changes in the SSP1-2.6 and SSP5-8.5 scenarios are likely to impact each ecosystem service in the future. The justification for the contribution level of each ecosystem service for both habitats is outlined in Sections 3.11.1–3.11.5. In Section 3.11.6, we discuss the impacts of climate change on AIMPA biodiversity. Finally, in Section 3.11.7, we describe how the changing climate and changing biodiversity is likely to affect ecosystem services around the AIMPA.

3.11.1. Maintenance of Genetic Diversity

The AIMPA's shallow subtidal zone harbors a large number of endemic algae (Tsiamis et al., 2017), fish (Wirtz et al., 2017) and invertebrates (Barnes, 2017), with 8.3% of all fish species endemic, and only 12% of its species shared with its nearest neighbor, Saint Helena (Wirtz et al., 2017). With this isolation, the AIMPA's shallow water endemic species are unlikely to be able to migrate to neighboring habitats if conditions were to become unfavorable. Due to this high level of endemism, the AIMPA's shallow sub-littoral provides a significant contribution (score: 3) to the maintenance of genetic diversity.

The AIMPA's pelagic zone is home to an abundance of marine megafauna including sharks, tunas, billfish, rays and cetaceans (Thompson et al., 2021). Many of these are threatened species (International Union for Conservation of Nature, 2023), and the creation of the AIMPA may play a substantial role in the protection of these species. As such, the pelagic zone also provides a significant contribution (score: 3) to the maintenance of genetic diversity ecosystem service.
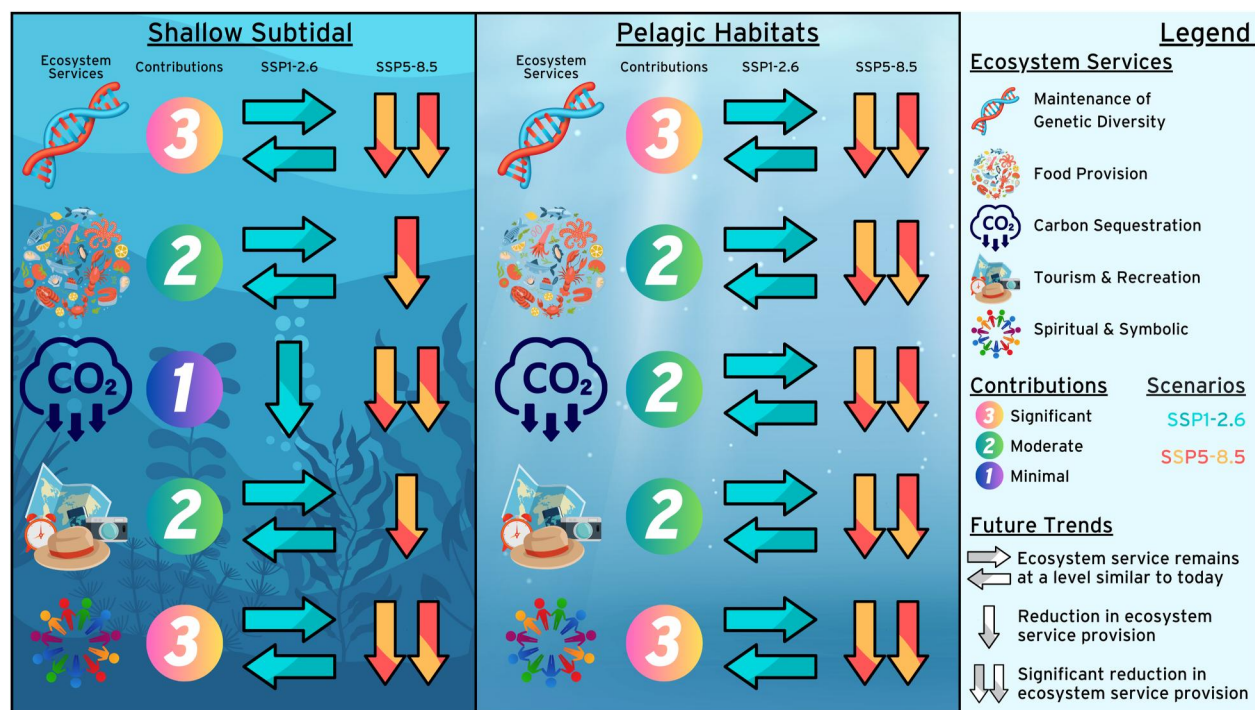
Figure 13. The Ascension Island pelagic and shallow subtidal ecosystem services, their contribution levels ranked 1–3, and the projected effect of the SSP1-2.6 (blue–green arrows) and SSP5-8.5 scenarios (orange–red arrows) on these ecosystem services.

3.11.2. Food Provision

Seafood from the subtidal zone is a large component of islanders diet and fish such as groupers, tunas and jacks can be caught by small scale local fishers from the shore of Ascension Island (McDonald, 2012). There is also local demand for the spiny lobster (Ascension Island Government, 2015).

In the AIMPA pelagic zone, small-scale extractive fisheries are able to operate within 12 NM of the shore, and pelagic fish such as tuna and jacks provide an important food source for islanders (Ascension Island Government, 2021b). The lack of reproductively active yellowfin tuna within the AIMPA (Richardson et al., 2018), suggests that the AIMPA is not a spawning site and there is unlikely to be a spillover effect for this species.

Both the pelagic and subtidal habitat ecosystem service contributions are expected to be moderate (score: 2). This is because these locally caught fish provide an important role in the diet of the islanders, but are not internationally exported.

3.11.3. Carbon Sequestration

In the AIMPA's shallow subtidal zone, there is a paucity of filamentous and fleshy algae, except in inaccessible nooks and crannies. This is because the locally abundant black triggerfish (*Melichthys Niger*) actively graze on the algae (Price & John, 1980). In addition, coralline algae dominate the shallow sublittoral landscape (Tsiamis et al., 2017). These algae will contribute to carbon sequestration (Trevathan-Tackett et al., 2015), but they are extremely susceptible to ocean acidification (Cornwall et al., 2022), and the lack of blue carbon habitats such as seagrasses or mangroves around Ascension island suggest that the AIMPA's subtidal carbon sequestration ecosystem service contribution is minimal (score: 1) compared to other shallow water habitats. For instance, the global carbon sequestration rates of mangroves forests is 13.5 PgC yr^{-1} (Alongi, 2012) or the global carbon stock of seagrasses is 19.9 PgC (Fourqurean et al., 2012).

In the pelagic zone, the food web plays an important role in the biological pump, with carbon transported from the ocean surface to the deep sea through the sinking of particles such as zooplankton, fecal pellets, marine snow, and phytoplankton detritus (Turner, 2015). The global total carbon export from the Biological Carbon Pump was

calculated to be approximately 10.2 PgC yr^{-1} (Nowicki et al., 2022). In that work, the carbon export for the AIMPA is shown to be moderate with a value of 45–90 mgC m^{-2} d^{-1}. We estimate the annual export of the entire AIMPA is between 7.3 and 14.6 TgC yr^{-1}. As such, the AIMPA is responsible for between 0.07% and 0.14% of the oceans export while accounting for 0.12% of the area. The sinking of large fish and marine megafauna into the deep sea in the AIMPA is also expected to be a proportionally large carbon sink, due to the protected status and the lack of industrial fishing (Mariani et al., 2020). However, the estimated global carbon stock of marine vertebrates is only 0.7 Pg (Bar-On et al., 2018), so we did not consider this to be a significant contribution to sequestration. As such, we quantified the Pelagic ecosystem service contribution to carbon sequestration as moderate (score: 2).

3.11.4. Tourism and Recreation

Due to its remoteness, the Ascension Island has low tourism potential, which impacts the Tourism and recreation ecosystem services in both the shallow subtidal and pelagic habitats. Whilst tourism was paused on the island due to the lack of a suitable runway at the airport and a limited number of commercial flights, the new runway was completed recently in 2023 (Royal Air Force, 2023). Tourism opportunities may return in the future if the airport were to open additional commercial routes. While cruise ships and small private yachts are a source of tourism, they are relatively infrequent (Hardman et al., 2022).

Recreational fishing and sports fishing occurs from small boats around both the shallow subtidal and pelagic zones and is a large part of the local culture (Ascension Island Government, 2021b). Three commercial sport fishing charters operated on the island prior to the closure of the runway in 2017 (Ascension Island Government, 2021b). However, due to the remoteness of the island, the low local population, and the limited tourist accommodation and services, their overall commercial contribution was small. In addition to fishing, other forms of marine recreation such as scuba diving and swimming are enjoyed by a large number of Ascension Island residents (Canelas et al., 2019). While tourism has historically been a small contributor to the islands economy, marine recreation is likely to play an important role for locals, so it's ecosystem service contribution is expected to be moderate for both habitats (score: 2).

3.11.5. Spiritual and Symbolic Cultural Services

Both the shallow subtidal and pelagic zones of the AIMPA are a habitat for sharks, tunas, turtles, endemic species and other marine life. The biodiversity, abundance and uniqueness of marine species in the UK Overseas Territories are known to provide social benefits to local populations (Carine et al., 2015), as well as boosting the natural heritage of the UK as a whole (Oldfield et al., 1999). This biodiversity has been shown to play a significant role in the natural heritage of Ascension Island's sister island Saint Helena, and due to their similarity, this is likely to be the case for Ascension as well (Canelas et al., 2019). In addition, the AIMPA's pelagic marine megafauna are iconic and of cultural importance both locally and internationally (Grose et al., 2020). As such, both the shallow subtidal and pelagic zones are considered as providing a significant contribution (score: 3) to spiritual and symbolic cultural services.

3.11.6. Impacts of Climate Change on AIMPA Biodiversity

In the AIMPA, the SST is projected to increase by 1.2°C in the SSP1-2.6 scenario MMM, and by 3.6°C in the SSP5-8.5 MMM by the year 2100 relative to the recent past (2000–2010). The sea surface pH is projected to decrease by −0.07 under the SSP1-2.6 scenario, and by −0.35 under the SSP5-8.5 scenario by the year 2100. By the year 2100 under both SSP1-2.6 and SSP5-8.5, the oxygen concentration at 500 m depth is projected to increase slightly and the IntPP MMM is projected to decrease slightly. However, we were unable to find any sensitivity studies that tested whether changes this small in oxygen concentration and primary production were sufficient to measurably impact the ecosystem service provision of either habitat.

Ocean acidification is likely to influence the dominance of primary producers and the biochemical composition of phytoplankton which will have repercussions up the food web due to changes in food quality and availability, although the repercussions of this are not currently well understood (Jin et al., 2020). In their microcosm experiment using phytoplankton sampled near the AIMPA at 7.5°S 28°W, Fernández-González et al. (2022) observed a decline in picophytoplankton biomass when they were subjected to a 3°C rise in temperature. This suggests that phytoplankton growth in the AIMPA may be particularly vulnerable to warming seas. In addition,

CMIP6 models project a significant change in the duration and intensity of marine heat waves in the equatorial Atlantic region (Qiu et al., 2021) which would likely further stress phytoplankton.

There are many lines of evidence that suggest that zooplankton production will decrease by the end of the century under the SSP5-8.5 projection. Firstly, SST warming is likely to alter zooplankton abundance and distribution, with an already notable poleward range expansion of zooplankton species in the NE Atlantic (Beaugrand et al., 2002), and an earlier annual peak in biomass of many species of zooplankton (Edwards & Richardson, 2004). Secondly, a pH decrease of −0.2, which is less severe than the −0.35 projected for the AIMPA, has been shown to reduce the abundance of zooplankton by two thirds at CO_2 seeps over tropical coral communities. Zooplankton abundance, fitness and survival have been shown to decrease when ocean acidification and ocean warming occur simultaneously (Garzke et al., 2017). In addition, copepod reproduction is adversely affected and nauplii mortality increases by 35% under the SSP5-8.5-like conditions (Lindeque et al., 2020). Finally, although zooplankton grazing is the largest source of uncertainty for marine carbon cycling in CMIP6 models (Rohr et al., 2023), most CMIP6 models are in agreement and project a decline in global zooplankton biomass (Petrik et al., 2022). Only one CMIP6 model in Petrik et al. (2022), CanESM5, projected a rise in global zooplankton biomass under the SSP5-8.5 scenario. In that study, CanESM5 underestimated the historic zooplankton biomass by an order of magnitude but also projected a significant rise in zooplankton food sources (via surface chlorophyll concentration) over the same period. Under the SSP5-8.5 scenario a decrease in zooplankton abundance and biomass is highly likely and would lead to a reduction in energy availability for species in higher trophic levels. The changes projected under the SSP1-2.6 scenario are not anticipated to cause the same large changes in energy availability.

Coralline algae dominates the shallow subtidal habitats of Ascension Island. In tropical ecosystems, coralline algae is thought to enhance biodiversity by providing a suitable substrate for attachment or by increasing recruitment through providing chemical cues that trigger larval metamorphosis (McCoy & Kamenos, 2015). Due to the large numbers of grazing black triggerfish consuming algae (Price & John, 1980), fleshy or filamentous algae are unlikely to replace coralline algae under future climate. In addition, ocean acidification and pH fluctuations have been shown to have a detrimental effect on the growth and development of coralline algal recruits (Roleda et al., 2015). While it is a cold-water coralline algae, the growth rate and cellular integrity of *Lithothamnion glaciale* have been shown to decrease under a high CO_2 emission scenario similar to SSP5-8.5 (Ragazzola et al., 2012), and a combination of ocean acidification and increased temperature led to tissue necrosis and net dissolution (Martin & Gattuso, 2009). Even in the SSP1-2.6 projection, there may be negative impacts on coralline algae like *Lithothamnion glaciale* by the year 2100 as they are highly susceptible to small pH changes (Bradassi et al., 2013).

There are many species of invertebrates in the AIMPAs shallow subtidal habitat, including mobile crustaceans, molluscs, and echinoderms (Brown et al., 2016), and encrusting species of fauna such as bryozoans, many of which are endemic (Barnes, 2017). The thermal tolerance of most of these species is unknown, but the tropical spiny lobster of the *Palinuridae* family has been well studied and is likely to suffer under the SSP5-8.5 projection. This is because temperatures above 32°C significantly reduce juvenile survival rates (Lellis & Russell, 1990), alter chemosensory behavior (Ross & Behringer, 2019), and decrease growth rates (Uy et al., 2023). Furthermore, CMIP6 models project significant increases in the duration and intensity of marine heat waves in the equatorial Atlantic region (Qiu et al., 2021), especially under the SSP5-8.5 projection, and marine heat waves have been show to have severe impacts on benthic invertebrates (Garrabou et al., 2019). Calcifying invertebrates such as molluscs, echinoderms and bryozoans are particularly vulnerable to acidification (Dupont et al., 2010; Parker et al., 2013; Smith, 2009) and ocean warming is likely to exacerbate that impact (Rodolfo-Metalpa et al., 2011; S.-A. Watson et al., 2012). Whilst ocean acidification often elicits species-specific responses, any sub-lethal effects are likely to lead to significant threats to marine organisms. There is no evidence that the smaller changes expected under the SSP1-2.6 projection will affect the AIMPA's invertebrate population, although those species living at the limit of their thermal or pH tolerance may be impacted.

The global marine ecosystem models in the Fisheries and Marine Ecosystem Model Intercomparison Project (Fish-MIP) projected a decline in marine animal biomass in the equatorial Atlantic of approximately 50% between 1990–1999 and 2090–2999 under the SSP5-8.5 scenario (Tittensor et al., 2021). Counter-intuitively, habitat suitability for certain tuna species may actually increase around Ascension Island between now and 2080 under the RCP-8.5 scenario (which is comparable to SSP5-8.5) (Townhill et al., 2021). However, as zooplankton

abundance is suspected to decrease under the SSP5-8.5 projection (Petrik et al., 2022), any positive changes in habitat suitability due to climate change for tuna or other pelagic fishes will likely be lost through loss of energy at the base of the food chain. Similarly, fish that live in the shallow subtidal are likely to be negatively affected by the decrease in abundance of coralline algae and invertebrates projected in SSP5-8.5. Ocean acidification is likely to further reduce the fitness of fish through the energetic trade-off of coping with elevated blood carbon dioxide levels (hypercapnia) (Heuer & Grosell, 2014) and warming temperatures are likely to impact any of the fish living within 3°C of their thermal limit. This may lead to a loss of endemic species, as Ascension Island's isolation prevents migration of shallow water species.

Globally, one-third of marine megafauna species are at risk of extinction; but due to their size and mobility, they are difficult to study using traditional experimental or modeling approaches (Pimiento et al., 2020). Ascension Island is a nesting area for a large population of green turtles which migrate from the Brazilian coastline to Ascension Island to reproduce during a 4,400 km round trip (Hays et al., 2002). Whilst the mean SST is not expected to exceed the green turtles usual temperature range of 25–35°C (Kraus & Jackson, 1980) under either scenario, climate change could impact turtles at other life stages. Sex determination in the nest is influenced by temperature, with an increasing proportion of females linked to increasing temperatures (Poloczanska et al., 2009), and higher temperatures associated with reduced hatching success (Tilley et al., 2019; Yao et al., 2022). Climate change is expected to alter the distribution of marine megafauna such as elasmobranchs (sharks and rays) and cetaceans (marine mammals) with species increasingly moving poleward alongside the range shift of their prey (Grose et al., 2020). Manta rays appear to migrate to cooler waters during ENSO events, suggesting that these animals may be sensitive to large fluctuations in temperature, although it is unknown whether this change in distribution is due to the temperature itself, changes in prey abundance, or other co-varying environmental variables (Beale et al., 2019). Manta rays may avoid the AIMPA during marine heat waves, which are likely to become more frequent under the SSP5-8.5 scenario. In contrast, whale sharks appear to frequent waters of up to 36°C in the Arabian Gulf, suggesting these species thrive in warm temperatures (Robinson et al., 2017). Few studies exist that show a direct impact of ocean acidification on megafauna. However, the megafauna's food availability is likely to be negatively impacted by the ocean acidification projected in the SSP5-8.5 scenario as described above, which may well lead to a reduction in marine megafauna.

3.11.7. Impacts of Climate Change on AIMPA Ecosystem Services

We found no evidence that the projected temperature and pH changes under the SSP1-2.6 projection would result in a loss of ecosystem services in either habitat by the year 2100. Both shallow subtidal and pelagic zone ecosystem services are likely to remain at a level similar to today (trend: ↔), with the exception of a decrease in coralline algae, reducing carbon sequestration in the shallow subtidal (trend: ↓). This means that a significant part of the AIMPA ecosystem services may be preserved if future emissions and warming follow the SSP1-2.6 pathway.

In the AIMPA shallow subtidal zone, the increase in temperature and decrease in pH by the year 2100 under the SSP5-8.5 projection is likely to be the key driver of ecosystem service reduction. The maintenance of genetic diversity may be significantly impacted through a loss of calcifying species and species living near their thermal limit (trend: ↓ ↓). This impact is also likely to lead to a similar decrease in food provision (trend: ↓). Carbon sequestration in the shallow subtidal zone will be significantly negatively affected under the SSP5-8.5 projection (trend: ↓ ↓), as coralline algae is extremely susceptible to a decrease in pH. The tourism and recreation ecosystem services are all likely to decrease (trend: ↓) with the loss of species abundance and biodiversity and subsequent impacts on fishing and marine recreation projected in the AIMPA shallow subtidal zone by the year 2100 under the SSP5-8.5 projection. The spiritual and symbolic ecosystem services are all likely to significantly decrease (trend: ↓ ↓) as endemic marine species, biodiversity and natural heritage are projected to decline in the AIMPA shallow subtidal zone by the year 2100 under the SSP5-8.5 projection.

In the pelagic zone under the SSP5-8.5 projection at the year 2100, a significant rise in temperature and acidification, an increase in the intensity and duration of marine heat waves, a decline in local phytoplankton biomass due to their vulnerability to warming, a global decline in zooplankton biomass, and a 50% decline in marine animal biomass in the equatorial Atlantic all contribute to a significant decrease in pelagic zone ecosystem services. The loss of phytoplankton, zooplankton and marine animal biomass significantly reduces the maintenance of genetic diversity ecosystem service (trend: ↓ ↓). Any decrease in primary or secondary production will

likely lead to a decrease in carbon sequestration through declines in the sinking of particles such as zooplankton, fecal pellets, marine snow, and phytoplankton detritus (trend: ↓ ↓). A decrease in zooplankton would lead to food becoming limiting for their predators, leading to a decrease in fish, which directly reduces the food provision ecosystem service (trend: ↓ ↓). While there is some evidence that the habitat suitability of some species of tuna and whale sharks will expand under future warming conditions in the SSP5-8.5 projection at the year 2100, it is likely that their food sources will not benefit from the same conditions. Similarly, other species such as green turtles and manta rays are likely to be negatively impacted by warming, acidification and loss of prey. The reduction in marine megafauna and the reduction in pelagic fish would lead to a significant decline in the pelagic zone under the SSP5-8.5 projection in both cultural ecosystem service categories: tourism and recreation, and spiritual and symbolic (trend: ↓ ↓).

4. Discussion

In this section, firstly, we summarize our main results and explain how these results link together, we then explain some of the implications and consequences of this work. Finally, we discuss the limitations and some potential extensions for this work.

4.1. Summary of Main Results

The CMIP6 MMMs project that the AIMPA region will become warmer, more saline, more acidic, with less nutrients at the surface, and likely to have lower chlorophyll concentration and less primary production by the middle of the 21st century, as summarized in Figure 2. This is likely to result in a decline in zooplankton, fish, and marine megafauna populations. In most cases, these changes are more extreme in the future scenarios that include stronger emission of greenhouse gases and more significant climate change. Toward the end of the projection period, these changes become more extreme and the scenarios diverge further.

The process through which these changes will occur begins with the rise in atmospheric CO_2 and other greenhouse gases, which capture addition solar radiation in the atmosphere, raising the Earth's radiative forcing. In the AIMPA, the increase in radiative forcing from the atmosphere will warm the ocean, as shown in the MMM temperature in Figure 3. A rise in precipitation (Tebaldi et al., 2021) and an increase in surface evaporation (Douville et al., 2021) are also projected for the region. Both of these factors influence salinity in opposite directions, but the CMIP6 MMM projects a rise in the AIMPA's surface salinity in Figure 4. The changes in temperature and salinity will influence the physical circulation of the equatorial Atlantic, resulting in a shallowing of the MLD in Figure 5 and a weakening of the AEU, shown in Figure 12. The projected decline in the AEU reflects an overall weakening in the wider Atlantic and local current systems (Eyring et al., 2021; Richter & Tokinaga, 2022). The combination of warmer surface layers, increased stratification, and reductions in circulation, will impact the marine biogeochemistry of the region. Less nutrient-rich deep water will be mixed into the surface layers, and the average nutrient concentration at the surface will decline, as shown in Figures 8 and 9. The decline in nutrients and primary production began around 1995 and likely has already had an impact on the AIMPA ecosystem. With less nutrients available in the well-lit surface layers, the chlorophyll concentration and primary production decrease, shown in Figures 10 and 11. Furthermore, ocean acidification shown in Figure 7, caused by a higher concentration of atmospheric carbon dioxide being absorbed by the surface layers, is likely to add further stress to marine organisms.

Several locally important species of marine invertebrates, fish and megafauna are likely to be severely impacted by the projected warming in the SSP5-8.5 scenario (Beale et al., 2019; Heuer & Grosell, 2014; Pimiento et al., 2020; Poloczanska et al., 2009; Tittensor et al., 2021) and both the intensity and duration of marine heat waves in the region are likely to increase in the equatorial Atlantic (Qiu et al., 2021). As such, under the SSP5-8.5 projection, the AIMPA's ecosystem may become simplified and with reduced biodiversity. The richness of the AIMPAs marine biodiversity has a significant impact on the ecosystem services, influencing the maintenance of genetic diversity, food provision, tourism & recreation and spiritual & symbolic ecosystem services as summarized in Figure 13. Both the subtidal and pelagic habitats ecosystem services provision are likely to remain at a level similar to today under the SSP1-2.6 scenario, but there are likely to be reductions or significant reductions under the SSP5-8.5 scenario.

4.2. AEU and Oxygen Concentration

Our analysis of the evolution of the AEU flow indicates a substantial scenario-dependent weakening of the current over the coming century. The bulk of the changes are projected to occur in the second half of the century and the strongest weakening occurs in the SSP5-8.5 scenario. All projections consistently point to a reduction in the mean AEU flow superimposed onto its variability. The natural portion of the AEU variability is linked to climatic cycles, but can be substantial to the point of obscuring the climate change signal for short observation periods. This effect can be seen in Figure 12a observational data. The AEU is one of the current that brings oxygenated surface water to the tropical subsurface layer (Duteil et al., 2014; Hahn et al., 2017; Oschlies et al., 2018). In addition, decadal and multi-decadal variations in oxygen concentration in the tropical Atlantic result mainly from the variability in currents redistributing oxygen (Brandt et al., 2015; Montes et al., 2016). As a consequence, the projected AEU weakening will likely cause a decline in the oxygen concentration in the tropical subsurface layer, reducing the habitat's suitability for tropical pelagic fish.

OMZs are regions where the oxygen concentration is below 80 mmol m^{-3} (Bopp et al., 2013; Cocco et al., 2013). OMZs are generally unsuitable habitat for active, high-metabolic-rate pelagic fishes (Stramma et al., 2012). While several models are already below the OMZ cut off value at 500 m in the historical simulations, this is not seen in the observational data. Of the models that fall within the observational range (89–113 mmol m^{-3}), some project a rise while others project a decline in oxygen concentration at 500 m. Those models that project a decline from the observed range in the annual mean oxygen concentration at 500 m start the historical period around 95–105 mmol m^{-3} and fall to 85–95 mmol m^{-3} by the mid-century future period. Their decline does not approach the OMZ cut-off value of 80 mmol m^{-3} until the year 2070. In addition, the models that project a decline from the observed range are a small subset of the ensemble, and the overall MMM projects a rise in oxygen concentration. Of the three models that erroneously included an OMZ in the AIMPA at 500m in the historical period (1850–2015), all three project a rise in oxygenation in all scenarios before the year 2050. Therefore, it is unlikely that the MPA will develop an OMZ by the mid-century future period.

The ecosystem services assessment was performed using the change in the decadal means between 2000–2010 and 2090–2100. While all ecosystem services were projected to be negatively impacted under the SSP5-8.5 projection, the assessment would likely be even more severe were higher frequency data used. This is because monthly and daily model data would likely project a significantly more diverse range of variability, and include more extreme temperatures. For instance, it is known that marine heatwaves are likely to increase in frequency and severity (Benedetti-Cecchi, 2021), and several important species in the AIMPA are sensitive to temperature, notably green turtles, manta rays, tropical spiny lobster and other invertebrates. This may well lead to even more significant decreases in ecosystem service provision, particularly the maintenance of genetic diversity, food provision, tourism & recreation and spiritual & symbolic ecosystem services.

4.3. The Role of Marine Protection in Projection

The changes to the marine environment that are projected by CMIP6 models inside the AIMPA are likely to have significant consequences for local marine life. CMIP6 models are unable to directly determine the value of the no-take MPA protected status in buffering the impact of the changing climate. However, there is a significant body of evidence showing that overfishing has a significant negative effect on ecosystem health (Coll et al., 2008; Pikitch, 2012) and the absence of overfishing is likely to improve the AIMPA's capacity to mitigate the worst effects of the changing climate relative to regions where over-fishing still occurs (Jaureguiberry et al., 2022; Pikitch, 2012).

One of the key recommendations for global marine conservation is to expand the scope and the coverage of MPAs (Jefferson et al., 2021; O'Leary et al., 2016) in order to protect biodiversity, preserve ecosystem services, and achieve socioeconomic priorities. The recently ratified High Seas Treaty (United Nations General Assembly, 2017) has allowed the creation of MPAs outside national marine boundaries. For the first time, there is a pathway to create MPAs in the 60% of the ocean that was previously left open to unlimited exploitation. Choosing a location for a new MPAs is a complicated question, impacted by local biodiversity, historical fishing rights, and other regional socio-economic and political factors. However, in the near future, it may be possible to extend the AIMPA outside the Island's EEZ to create a protected corridor between the AIMPA and the other southern Atlantic MPAs. While the AIMPA's shallow water endemic species are unlikely to be able to migrate to neighboring habitats, an expansion of protected pelagic habitat could be beneficial to the AIMPA's pelagic species

that are also present in Saint Helena (Wirtz et al., 2017). However, further work would be needed to determine the extent either MPA would benefit from a protected corridor in the high seas.

4.4. The Tension Between Pragmatic Policy and CMIP6 Projections

The purpose of this study has been to assist local policymakers with decision making (de Mora et al., 2022). Many of the fields included here do not show a significant divergence between scenarios in the 2040–2050 in this region. This is a direct consequence of the choices defined in the scenario forcing, which reflects the inertia and complexity of changing the global socio-economic systems over the next three decades.

These scenarios were based on feasible emission projections, and were expected to result in a global mean surface warming of between 1.5 and 2°C in the year 2050 (O'Neill et al., 2016; Riahi et al., 2017). However the warming was never expected to be evenly distributed across the Earths surface. Under all climate change projections, the polar regions warm more than the tropics and the land surface temperature rises more than the sea surface (Tebaldi et al., 2021). For this reason, the temperatures of equatorial ocean surface of the AIMPA do not diverge significantly in the years 2040–2050 between these four scenarios. However, the second half of the century shows a much wider range of behaviors. The projected temperature, salinity and pH, all show significant divergences between scenarios after 2050.

From a policymaker perspective, the narrow range of projection between scenarios in the near future allows for a more precise projection of the future of the AIMPA. In the year 2100, the AIMPA may warm by between 1.2 and 3.6°C, which is a huge range and highly scenario-dependant. However, by the year 2050, the warming is much narrowly defined: 0.8–1.1°C. This narrower range may allow for policy to be more targeted for this time period, re-framing climate change from a nebulous threat in the distant future to a local pressure with real impacts and real solutions (S. Weber et al., 2023).

4.5. Limitations and Extensions

The analysis presented here has a few limitations that could be addressed in future iterations of this work. When focusing on the ensemble mean, some of the variability seen in individual models is lost. This effect can be seen especially in the MLD, nitrate and phosphate concentration data. Similarly, individual models in the ensemble may project opposing directions of travel for the future, as for instance in the chlorophyll and oxygen concentration data. In some cases, a single model with a substantial change can outbalance the consensus of the other models, for instance in the chlorophyll concentration data. In nature, several factors impact chlorophyll concentration: the primary production, the total biomass of each phytoplankton functional type, the ratio of carbon to chlorophyll within phytoplankton, the level of mixotrohpy, phytoplankton mortality, the sinking rate of phytoplankton and detritus, and grazing pressure. Each of the CMIP6 models will have different implicit or explicit implementations of these factors in their model, and it is the interplay between them that result in the total chlorophyll concentration. In addition, the advent of satellite observations resulted in surface chlorophyll concentration being one of the data sets with the most observations (Jackson et al., 2022). This makes accurate reproductions of historical chlorophyll concentration behavior one of the most challenging aspects of marine biogeochemistry modeling.

CMIP6 models typically have a resolution of approximately 1° by 1°. As such, the AIMPA is often only represented by a small number of model pixels. This can be as little as 6 or 7 pixels in the zonal direction in the models native resolutions. In effect, the circular AIMPA is 740 km in diameter, but many CMIP6 model pixels are approximately 100–120 km wide at this latitude. Note that global models typically have a band of higher meridional resolution near the equator (Hewitt et al., 2010). In either case, the AIMPA is relatively poorly spatially resolved in most CMIP6 model grids and that we were unable to use these models to investigate the spatial variability within the AIMPA. Policymakers would likely benefit from knowledge about locations inside the AIMPA that are more susceptible to marine heat waves, ocean acidification hot spots, and deoxygenation. However, it is not possible to use the observational record, or our methodology to spatially resolve the ecosystem behavior within the AIMPA. In addition, Ascension Island itself is approximately 0.1° in diameter and can not be represented even as a seamount, at the typical CMIP6 model resolution. Similarly, the coarse resolution model grids in CMIP6 means that they can not accurately capture important local circulation patterns. Moving to higher resolutions ocean models may occur in future generations of CMIP which would help resolve the small scale features around the AIMPA. However, in the short term, there will likely be a trade off between resolution and

complexity as increasing the number of advected tracers may raise the computational cost of the marine component of these models (Balaji et al., 2017). Alternatively, a bespoke higher resolution regional model of the central Atlantic may allow a focus on the AIMPA.

The range of marine biogeochemistry models in CMIP6 is fairly limited to relatively simple and moderate trophic complexity models with modest skill in capturing regional patterns (Kwiatkowski et al., 2020; Tagliabue et al., 2021). Several CMIP6 models use two or fewer phytoplankton functional types (Rohr et al., 2023), which may not be sufficient to capture dynamic blooms and trophic cascades (Hashioka et al., 2013), as reflected in the chlorophyll concentration climatology in Figure 10b. In addition, ESMs try to capture global plankton communities and not those that may be regionally important.

As shown in Table 1, the number of models and ensemble members varies significantly between analyses and scenarios. Future studies could objectively judge models according to their historical performance and use this information to weight the final mean as in Brunner et al. (2020). For instance, future studies may choose to favor models that reproduce physical features like SST or MLD from observations. Alternatively, we could have removed models that are inappropriately parameterized for marine biogeochemistry analysis by investigating each model's internal structure. For instance, future studies may choose to include only models that have sufficiently complex marine biogeochemistry, such as two or more phytoplankton functional types, variable stoichiometry, nitrogen fixation, a fully resolved bacterial functional type, or higher trophic levels. Additionally, future studies could use pre-industrial control simulations to de-drift models or calculate precise anomalies over the entire historical and future time periods.

The authors are not aware of any CMIP6 model or forcing scenario that explicitly include either fish or fishing behavior. For instance, Séférian et al. (2020) was a broad review of the state of CMIP marine biogeochemistry models and did not include any models that explicitly modeled fish. This is in part due to the relative simplicity of the CMIP6 marine biogeochemistry models and the complexity needed to model fisheries. A bespoke high-resolution simulation of the marine ecosystem in the region could be made using a model with a state-of-the-art complexity level, such as ERSEM (Butenschön et al., 2016; Vichi et al., 2015), would allow a more in-depth analysis of the behavior in the AIMPA. Similarly, a 1D water column model could be generated for the AIMPA at lower cost, but use a more complex marine biogeochemical model. Alternatively, it could be possible to use CMIP6 data to drive an offline fish model for the AIMPA as in Tittensor et al. (2018, 2021). In addition to the higher costs of developing a bespoke model, there would also be no option to compute a MMM.

While fish are not explicitly included in CMIP6 models, they are included implicitly through top down control on zooplankton via grazing pressure or mortality rates. Protected status may impact the ecosystem in ways which can not be included in such a model. For instance, zooplankton grazing pressure and mortality rate parameterizations may differ in an overfished environment compared to a protected marine environment. In practice, these parameters are likely to be hardwired global settings in the models which can not be adjusted to take into account for local variability like MPAs. Protected status may also impact other implicitly modeled features, such as megafauna-mediated nutrient recycling, which could potentially impact primary production, the microbial carbon pump, and hence nutrient concentrations and the wider carbon cycle (Gross, 2016; Polimene et al., 2016; Roman & McCarthy, 2010).

An over-fished marine environment may be a net carbon source (Atwood et al., 2024) while a fully protected marine ecosystem may be a carbon sink (Jankowska et al., 2022). However, in CMIP6 ScenarioMIP simulations, the atmospheric CO_2 and other greenhouse gases of each scenario is identical between models and determined in advance. This means that carbon is not conserved, and there is no feedback between the creation of MPAs and the CO_2 or methane concentration. The existence of MPAs may be implicitly included in the forcing scenario, but ScenarioMIP's format and forcing was decided in 2015, several years before the AIMPA was created in 2019 and before the 30% by 2030 protection target was established (Woodley et al., 2019). This means that any positive or negative feedbacks that may occur due to the existence or absence of these MPAs will not be included in the CMIP6 simulations. A solution to this problem would be to instead use emissions-based simulations, where CO_2 emissions are fixed, instead of concentration driven scenarios. In these simulations, the total carbon in the model is conserved and is free to move between the atmosphere and ocean. Such simulations could potentially be set up to study the impact of MPA creation on the wider carbon cycle.

The analysis was limited to the data that was available at the time that the work was performed. This may not include all fields from ensemble members from all CMIP6 models. In addition, several models whose data was present were not accessible due to technical problems, such as non-standard formatting or gaps in the time series. When designing the experiment, we attempted to maximize the number of contributing models for each analysis, but additional CMIP models are likely to be available when new or revised data sets are published in the future.

While the Atlantic Meridional Transect program cruise has passed through the AIMPA on several occasions (Rees et al., 2024), there is no regular long-term marine biogeochemistry data set for the region. The scarcity of the in situ observational record in the region has limited the quality of the observational data set products available. A long-term monitoring program inside the AIMPA and in other MPAs, would provide regular data at a range of depths which could help validate models and provide insight into both the historic and future health of the protected ecosystems.

While methodologies exist to perform an ecosystem services analysis for the deep sea benthic environment (e.g., Armstrong et al., 2012), there was insufficient data available for a full sensitivity analysis of the deep sea habitats. In addition, most of the CMA analyses shown here show very little change between the recent past and the mid-century future at the AIMPA seafloor in the anomaly profiles in pane d. Further refinements could include assessing intertidal habitats and ecosystem services more thoroughly. Further work could also include modeling ecosystems service provision under climate change using and modeling indicator outputs (Queirós et al., 2021), but this would need another set of modeling approaches in addition to the work carried out here.

Finally, a possible extension of this work could focus on the ecological impacts of the projected changes inside the AIMPA. These additional metrics could include changes in the plankton and nekton biomass and emergent properties such as phytoplankton community structure, stoichiometry or the carbon to chlorophyll ratio (de Mora et al., 2016).

5. Conclusions

An analysis of the CMIP6 climate projections for the AIMPA was presented for the first time. We showed both the historic period and four future climate scenarios using a large ensemble of ESMs. The AIMPA region was projected to become warmer, more saline, more acidic, with lower surface nutrient concentrations, lower chlorophyll concentration and less primary production. In most cases, these changes were more extreme in the future scenarios that are associated with the stronger emission of greenhouse gases. Most of the MMM projections did not diverge significantly before the year 2050 in this region, but almost all variables analyzed here showed a wide range of scenario-dependent behavior in the second half of the century. Even in the most sustainable projection, SSP1-2.6, there was still evidence that these changes will likely occur. However, the scale and severity of the damage to the AIMPA and its ecosystem services under the enhanced fossil fuel usage scenario, SSP5-8.5, should add further urgency to the case for a reduction in global emissions and transition away from fossil fuels.

The development of climate models is an on-going challenge for the scientific community, and models are constantly being improved to become more accurate and realistic. The upcoming CMIP7 is likely to include more higher resolution models and scenarios, more marine processes and ecosystem complexity and improvements in process modeling relative to the current generation. Future work could focus on predicting climate change responses for an even wider range of species and habitats, using updated model outputs, and may be able to spatially resolve the ecosystem behavior within the AIMPA. Similarly, this work would not be possible without on-going international efforts to generate global scale data sets of observations, in the Wold Ocean Atlas data set, the Global Ocean Data Analysis Project, the European Space Agency Climate Change Initiative and the Tropical Atlantic Observing System. These observations form the bedrock of our projection analysis and should continue to be supported in the future.

The work was part of the CRACAB project (S. Weber et al., 2023). The CRACAB project used an island-wide approach to generate projections of the most serious impacts of climate change on the Ascension Island and the AIMPA. By providing better information about the future of the Ascension islands marine environment, the project re-framed climate change from a nebulous threat to a local pressure with real impacts and real solutions. The region-specific information generated by the project was able to capture the attention of policy makers, allowing quantitative measures of risk and impact to be incorporated into the Ascension Island Governments strategies and adaptation plans. The sustainable adaptation measures that were recommended by the project

would build long-term resilience into Ascension Islands ecosystems strategy. In addition, the framework developed over the course of the CRACAB project is sufficiently flexible that it could be applied more widely in other MPAs. Existing, planned and potential MPAs policymakers could recreate this work to generate valuable bespoke projections of the future climate in their region. This would create a clear, thorough and pragmatic vision of the future of their local marine environment environment to support their decision making processes.

Data Availability Statement

This analysis was performed using the Earth System Model Evaluation Toolkit, ESMValTool. The code used in this manuscript and the data seen in figures are both available in the following Zenodo repository: de Mora ([2023](#)). The main ESMValTool recipes are in the `ai_mpa` and the `ai_mpa_2022/AEU` directories in `esmvaltool/recipes`. The main diagnostic script is `diagnostic_ai_plots.py` in the `esmvaltool/diag_scripts/ocean` directory. The up-to-date version of the base ESMValTool system is available on GitHub: https://github.com/ESMValGroup which includes more recent code, documentation, installation instructions and tutorials.

References

Alongi, D. M. (2012). Carbon sequestration in mangrove forests. *Carbon Management*, *3*(3), 313–322. https://doi.org/10.4155/cmt.12.20

Armstrong, C. W., Foley, N. S., Tinch, R., & van den Hove, S. (2012). Services from the deep: Steps towards valuation of deep sea goods and services. *Ecosystem Services*, *2*, 2–13. https://doi.org/10.1016/j.ecoser.2012.07.001

Ascension Island Government. (2015). The Ascension Island species action plan: Spiny lobster (Tech. Rep.). Retrieved from https://www.ascension.gov.ac/flora-and-fauna/spiny-lobster

Ascension Island Government. (2021a). The Ascension Island marine protected area management plan (Tech. Rep.). Retrieved from https://www.ascensionmpa.ac/management-plan

Ascension Island Government. (2021b). Ascension Island inshore fisheries strategy (Tech. Rep.). Retrieved from https://www.ascension.gov.ac/project/inshore-fisheries-management-strategy

Atwood, T. B., Romanou, A., DeVries, T., Lerner, P. E., Mayorga, J. S., Bradley, D., et al. (2024). Atmospheric CO_2 emissions and ocean acidification from bottom-trawling. *Frontiers in Marine Science*, *10*. https://doi.org/10.3389/fmars.2023.1125137

Balaji, V., Maisonnave, E., Zadeh, N., Lawrence, B. N., Biercamp, J., Fladrich, U., et al. (2017). CPMIP: Measurements of real computational performance of earth system models in CMIP6. *Geoscientific Model Development*, *10*(1), 19–34. https://doi.org/10.5194/gmd-10-19-2017

Balaji, V., Taylor, K. E., Juckes, M., Lawrence, B. N., Durack, P. J., Lautenschlager, M., et al. (2018). Requirements for a global data infrastructure in support of CMIP6. *Geoscientific Model Development*, *11*(9), 3659–3680. https://doi.org/10.5194/gmd-11-3659-2018

Barnes, D. K. (2017). Marine colonization and biodiversity at Ascension Island and remote islands. *Journal of the Marine Biological Association of the United Kingdom*, *97*(4), 771–782. https://doi.org/10.1017/S0025315415001526

Bar-On, Y. M., Phillips, R., & Milo, R. (2018). The biomass distribution on earth. *Proceedings of the National Academy of Sciences*, *115*(25), 6506–6511. https://doi.org/10.1073/pnas.1711842115

Bates, A. E., Cooke, R. S., Duncan, M. I., Edgar, G. J., Bruno, J. F., Benedetti-Cecchi, L., et al. (2019). Climate resilience in marine protected areas and the 'protection paradox'. *Biological Conservation*, *236*, 305–314. https://doi.org/10.1016/j.biocon.2019.05.005

Beale, C. S., Stewart, J. D., Setyawan, E., Sianipar, A. B., & Erdmann, M. V. (2019). Population dynamics of oceanic manta rays (Mobula birostris) in the Raja Ampat Archipelago, West Papua, Indonesia, and the impacts of the El Niño–Southern Oscillation on their movement ecology. *Diversity and Distributions*, *25*(9), 1472–1487. https://doi.org/10.1111/ddi.12962

Beaugrand, G., Reid, P. C., Ibañez, F., Lindley, J. A., & Edwards, M. (2002). Reorganization of north Atlantic marine copepod biodiversity and climate. *Science*, *296*(5573), 1692–1694. https://doi.org/10.1126/science.1071329

Behrenfeld, M. J., & Falkowski, P. G. (1997). A comsumer's guide to phytoplankton primary productivity models. *Limnology & Oceanography*, *42*(7), 1479–1491. https://doi.org/10.4319/lo.1997.42.7.1479

Benedetti-Cecchi, L. (2021). Complex networks of marine heatwaves reveal abrupt transitions in the global ocean. *Scientific Reports*, *11*(1), 1739. https://doi.org/10.1038/s41598-021-81369-3

Bopp, L., Resplandy, L., Orr, J. C., Doney, S. C., Dunne, J. P., Gehlen, M., et al. (2013). Multiple stressors of ocean ecosystems in the 21st century: Projections with CMIP5 models. *Biogeosciences*, *10*(10), 6225–6245. https://doi.org/10.5194/bg-10-6225-2013

Bourlès, B., Araujo, M., McPhaden, M. J., Brandt, P., Foltz, G. R., Lumpkin, R., et al. (2019). PIRATA: A sustained observing system for tropical Atlantic climate research and forecasting. *Earth and Space Science*, *6*(4), 577–616. https://doi.org/10.1029/2018EA000428

Bradassi, F., Cumani, F., Bressan, G., & Dupont, S. (2013). Early reproductive stages in the crustose coralline alga phymatolithon lenormandii are strongly affected by mild ocean acidification. *Marine Biology*, *160*(8), 2261–2269. https://doi.org/10.1007/s00227-013-2260-2

Brandt, P., Bange, H. W., Banyte, D., Dengler, M., Didwischus, S.-H., Fischer, T., et al. (2015). On the role of circulation and mixing in the ventilation of oxygen minimum zones with a focus on the eastern tropical North Atlantic. *Biogeosciences*, *12*(2), 489–512. https://doi.org/10.5194/bg-12-489-2015

Brandt, P., Hahn, J., Schmidtko, S., Tuchen, F. P., Kopte, R., Kiko, R., et al. (2021). Atlantic equatorial undercurrent intensification counteracts warming-induced deoxygenation. *Nature Geoscience*, *14*(5), 278–282. https://doi.org/10.1038/s41561-021-00716-1

Breitburg, D., Levin, L. A., Oschlies, A., Grégoire, M., Chavez, F. P., Conley, D. J., et al. (2018). Declining oxygen in the global ocean and coastal waters. *Science*, *359*(6371), eaam7240. https://doi.org/10.1126/science.aam7240

Brickle, P., Brown, J., Küpper, F. C., & Brewin, P. E. (2017). Biodiversity of the marine environment around Ascension Island, South Atlantic. *Journal of the Marine Biological Association of the United Kingdom*, *97*(4), 643–646. https://doi.org/10.1017/S0025315417001175

Broderick, A. C., Frauenstein, R., Glen, F., Hays, G. C., Jackson, A. L., Pelembe, T., et al. (2006). Are green turtles globally endangered? *Global Ecology and Biogeography*, *15*(1), 21–26. https://doi.org/10.1111/j.1466-822x.2006.00195.x

Brown, J., Downes, K., Mrowicki, R., & Richardson, A. (2016). New records of marine invertebrates from Ascension Island (central Atlantic). *Arquipelago - Life and Marine Sciences*, *33*, 71–79.

Brunner, L., Pendergrass, A. G., Lehner, F., Merrifield, A. L., Lorenz, R., & Knutti, R. (2020). Reduced global warming from CMIP6 projections when weighting models by performance and independence. *Earth System Dynamics*, *11*(4), 995–1012. https://doi.org/10.5194/esd-11-995-2020

Bruno, J. F., Bates, A. E., Cacciapaglia, C., Pike, E. P., Amstrup, S. C., van Hooidonk, R., et al. (2018). Climate change threatens the world's marine protected areas. *Nature Climate Change*, *8*(6), 499–503. https://doi.org/10.1038/s41558-018-0149-2

Butenschön, M., Clark, J., Aldridge, J. N., Allen, J. I., Artioli, Y., Blackford, J., et al. (2016). ERSEM 15.06: A generic model for marine biogeochemistry and the ecosystem dynamics of the lower trophic levels. *Geoscientific Model Development*, *9*(4), 1293–1339. https://doi.org/10.5194/gmd-9-1293-2016

Cabanes, C., Grouazel, A., von Schuckmann, K., Hamon, M., Turpin, V., Coatanoan, C., et al. (2013). The CORA dataset: Validation and diagnostics of in-situ ocean temperature and salinity measurements. *Ocean Science*, *9*(1), 1–18. https://doi.org/10.5194/os-9-1-2013

Canelas, J., Fish, R., Bormpoudakis, D., & Smith, N. (2019). *Cultural ecosystem services on Ascension Island. Natural capital in the UK's overseas territories report series – Supplementary report (South Atlantic region)* (Tech. Rep.). United Kingdom Overseas Territories Project. Retrieved from https://hub.jncc.gov.uk/assets/fd585938-685d-4e59-8f74-c2ce433071ab

Carine, M., Gray, A., Eaton, M., Hall, J., Havery, S., Scutt Phillips, J., et al. (2015). *Identifying evidence gaps to support the conservation and sustainable management of biodiversity and ecosystem services in the UK overseas Territories project reference number: BE0101 final report main project team executive summary* (Tech. Rep.). United Kingdom Overseas Territories Project.

Cocco, V., Joos, F., Steinacher, M., Frölicher, T. L., Bopp, L., Dunne, J., et al. (2013). Oxygen and indicators of stress for marine life in multi-model global warming projections. *Biogeosciences*, *10*(3), 1849–1868. Retrieved from https://bg.copernicus.org/articles/10/1849/2013/doi:10.5194/bg-10-1849-2013

Coll, M., Libralato, S., Tudela, S., Palomera, I., & Pranovi, F. (2008). Ecosystem overfishing in the ocean. *PLoS One*, *3*(12), 1–10. https://doi.org/10.1371/journal.pone.0003881

Cornwall, C. E., Harvey, B. P., Comeau, S., Cornwall, D. L., Hall-Spencer, J. M., Peña, V., et al. (2022). Understanding coralline algal responses to ocean acidification: Meta-analysis and synthesis. *Global Change Biology*, *28*(2), 362–374. https://doi.org/10.1111/gcb.15899

de Boyer Montegut, C., Madec, G., Fischer, A. S., Lazar, A., & Iudicone, D. (2004). Mixed layer depth over the global ocean: An examination of profile data and a profile-based climatology. *Journal of Geophysical Research*, *109*(C12). https://doi.org/10.1029/2004JC002378

Dee, D. P., Uppala, S. M., Simmons, A. J., Berrisford, P., Poli, P., Kobayashi, S., et al. (2011). The ERA-interim reanalysis: Configuration and performance of the data assimilation system. *Quarterly Journal of the Royal Meteorological Society*, *137*(656), 553–597. https://doi.org/10.1002/qj.828

de Mora, L. (2023). ESMValTool Ascension Island marine protection area projection analysis and supplemental data [Dataset, Software]. *Zenodo*. https://doi.org/10.5281/zenodo.8377128

de Mora, L., Butenschön, M., & Allen, J. I. (2016). The assessment of a global marine ecosystem model on the basis of emergent properties and ecosystem function: A case study with ERSEM. *Geoscientific Model Development*, *9*(1), 59–76. https://doi.org/10.5194/gmd-9-59-2016

de Mora, L., Galli, G., Artioli, Y., Weber, S., & Baum, D. (2022). Climate resilience and conservation of Ascension's biodiversity (CRACAB): CMIP6 forecast for the Ascension Island marine protected area and the wider region. Retrieved from https://ascension-climate.org/2022/04/25/climate-forecasting-for-the-ascension-island-marine-protected-area/

Douville, H., Raghavan, K., Renwick, J., Allan, R., Arias, P., Barlow, M., et al. (2021). Water cycle changes [Book Section]. In V. Masson-Delmotte, et al. (Eds.), *Climate change 2021: The physical science basis. Contribution of working Group I to the sixth assessment report of the intergovernmental panel on climate change* (pp. 1055–1210). https://doi.org/10.1017/9781009157896.010

Dupont, S., Ortega-Martínez, O., & Thorndyke, M. (2010). Impact of near-future ocean acidification on echinoderms. *Ecotoxicology*, *19*(3), 449–462. https://doi.org/10.1007/s10646-010-0463-6

du Pontavice, H., Gascuel, D., Reygondeau, G., Maureaud, A., & Cheung, W. W. L. (2020). Climate change undermines the global functioning of marine food webs. *Global Change Biology*, *26*(3), 1306–1318. https://doi.org/10.1111/gcb.14944

Duteil, O., Schwarzkopf, F. U., Böning, C. W., & Oschlies, A. (2014). Major role of the equatorial current system in setting oxygen levels in the eastern tropical Atlantic Ocean: A high-resolution model study. *Geophysical Research Letters*, *41*(6), 2033–2040. https://doi.org/10.1002/2013GL058888

Edwards, M., & Richardson, A. J. (2004). Impact of climate change on marine pelagic phenology and trophic mismatch. *Nature*, *430*(7002), 881–884. https://doi.org/10.1038/nature02808

Eyring, V., Bony, S., Meehl, G. A., Senior, C. A., Stevens, B., Stouffer, R. J., & Taylor, K. E. (2016). Overview of the coupled model inter-comparison project phase 6 (CMIP6) experimental design and organization. *Geoscientific Model Development*, *9*(5), 1937–1958. https://doi.org/10.5194/gmd-9-1937-2016

Eyring, V., Gillett, N., Achuta Rao, K., Barimalala, R., Barreiro Parrillo, M., Bellouin, N., et al. (2021). Human influence on the climate system [Book Section]. In V. Masson-Delmotte, et al. (Eds.), *Climate change 2021: The physical science basis. Contribution of working group I to the sixth assessment report of the intergovernmental panel on climate change* (pp. 423–552). https://doi.org/10.1017/9781009157896.005

Fernández-González, C., Tarran, G. A., Schuback, N., Woodward, E. M. S., Arístegui, J., & Marañón, E. (2022). Phytoplankton responses to changing temperature and nutrient availability are consistent across the tropical and subtropical Atlantic. *Communications Biology*, *5*(1), 1035. https://doi.org/10.1038/s42003-022-03971-z

Foltz, G., Brandt, P., Richter, I., Rodríguez-Fonseca, B., Hernandez, F., Dengler, M., et al. (2019). The tropical Atlantic observing system. *Frontiers in Marine Science*, *6*(206). https://doi.org/10.3389/fmars.2019.00206

Fourqurean, J. W., Duarte, C. M., Kennedy, H., Marbà, N., Holmer, M., Mateo, M. A., et al. (2012). Seagrass ecosystems as a globally significant carbon stock. *Nature Geoscience*, *5*(7), 505–509. https://doi.org/10.1038/ngeo1477

Fox-Kemper, B., Hewitt, H., Xiao, C., Aoalgeirsdottir, G., Drijfhout, S., Edwards, T., et al. (2021). Ocean, cryosphere and sea level change [Book Section]. In V. Masson-Delmotte et al. (Eds.), *Climate change 2021: The physical science basis. Contribution of working group I to the sixth assessment report of the intergovernmental panel on climate change* (pp. 1211–1362). https://doi.org/10.1017/9781009157896.011

Garcia, H., Weathers, K., Paver, C., Smolyar, I., Boyer, T., Locarnini, M., et al. (2018a). World Ocean Atlas 2018, Volume 3: Dissolved oxygen, apparent oxygen utilization, and dissolved oxygen saturation (Vol. *83*; Report). Retrieved from https://archimer.ifremer.fr/doc/00651/76337/

Garcia, H., Weathers, K., Paver, C., Smolyar, I., Boyer, T., Locarnini, M., et al. (2018b). World Ocean Atlas 2018 volume 4: Dissolved inorganic nutrients (phosphate, nitrate and nitrate+nitrite, silicate) (Vol. *84*; Report). Retrieved from https://archimer.ifremer.fr/doc/00651/76337/

Garrabou, J., Gómez-Gras, D., Ledoux, J.-B., Linares, C., Bensoussan, N., López-Sendino, P., et al. (2019). Collaborative database to track mass mortality events in the mediterranean sea. *Frontiers in Marine Science*, *6*. https://doi.org/10.3389/fmars.2019.00707

Garzke, J., Sommer, U., & Ismar, S. M. H. (2017). Is the chemical composition of biomass the agent by which ocean acidification influences on zooplankton ecology? *Aquatic Sciences*, *79*(3), 733–748. https://doi.org/10.1007/s00027-017-0532-5

GEBCO Compilation Group. (2023). General bathymetric chart of the oceans (GEBCO) 2023 grid. https://doi.org/10.5285/f98b053b-0cbc-6c23-e053-6c86abc0af7b

Giarolla, E., Siqueira, L. S. P., Bottino, M. J., Malagutti, M., Capistrano, V. B., & Nobre, P. (2015). Equatorial Atlantic Ocean dynamics in a coupled ocean–atmosphere model simulation. *Ocean Dynamics*, *65*(6), 831–843. https://doi.org/10.1007/s10236-015-0836-8

Godley, B. J., Broderick, A. C., & Hays, G. C. (2001). Nesting of green turtles (chelonia mydas) at Ascension Island, South Atlantic. *Biological Conservation*, *97*(2), 151–158. https://doi.org/10.1016/S0006-3207(00)00107-5

Graham, N. A. J., & McClanahan, T. R. (2013). The last call for marine wilderness? *BioScience*, *63*(5), 397–402. https://doi.org/10.1525/bio.2013.63.5.13

Griffies, S. M., Danabasoglu, G., Durack, P. J., Adcroft, A. J., Balaji, V., Böning, C. W., et al. (2016). Omip contribution to CMIP6: Experimental and diagnostic protocol for the physical component of the ocean model intercomparison project. *Geoscientific Model Development*, *9*(9), 3231–3296. https://doi.org/10.5194/gmd-9-3231-2016

Grose, S. O., Pendleton, L., Leathers, A., Cornish, A., & Waitai, S. (2020). Climate change will re-draw the map for marine megafauna and the people who depend on them. *Frontiers in Marine Science*, *7*. https://doi.org/10.3389/fmars.2020.00547

Gross, M. (2016). Megafauna moves nutrients uphill. *Current Biology*, *26*(1), R1–R5. https://doi.org/10.1016/j.cub.2015.12.028

Hahn, J., Brandt, P., Schmidtko, S., & Krahmann, G. (2017). Decadal oxygen change in the eastern tropical north Atlantic. *Ocean Science*, *13*(4), 551–576. https://doi.org/10.5194/os-13-551-2017

Hansen, G. J., Ban, N. C., Jones, M. L., Kaufman, L., Panes, H. M., Yasué, M., & Vincent, A. C. (2011). Hindsight in marine protected area selection: A comparison of ecological representation arising from opportunistic and systematic approaches. *Biological Conservation*, *144*(6), 1866–1875. https://doi.org/10.1016/j.biocon.2011.04.002

Hardman, E., Thomas, H. L., Baum, D., Clingham, E., Hobbs, R., Stamford, T., et al. (2022). Integrated marine management in the United Kingdom overseas Territories. *Frontiers in Marine Science*, *8*. https://doi.org/10.3389/fmars.2021.643729

Hashioka, T., Vogt, M., Yamanaka, Y., Le Quéré, C., Buitenhuis, E. T., Aita, M. N., et al. (2013). Phytoplankton competition during the spring bloom in four plankton functional type models. *Biogeosciences*, *10*(11), 6833–6850. https://doi.org/10.5194/bg-10-6833-2013

Hays, G. C., Broderick, A. C., Glen, F., & Godley, B. J. (2002). Change in body mass associated with long-term fasting in a marine reptile: The case of green turtles (Chelonia mydas) at Ascension Island. *Canadian Journal of Zoology*, *80*(7), 1299–1302. https://doi.org/10.1139/z02-110

Herrera, P. A., Marazuela, M. A., & Hofmann, T. (2022). Parameter estimation and uncertainty analysis in hydrological modeling. *WIREs Water*, *9*(1), e1569. https://doi.org/10.1002/wat2.1569

Heuer, R. M., & Grosell, M. (2014). Physiological impacts of elevated carbon dioxide and ocean acidification on fish. *American Journal of Physiology - Regulatory, Integrative and Comparative Physiology*, *307*(9), R1061–R1084. https://doi.org/10.1152/ajpregu.00064.2014

Hewitt, H., Copsey, D., Culverwell, I., Harris, C., Hill, R., Keen, A., et al. (2010). Design and implementation of the infrastructure of HadGEM3: The next-generation Met Office climate modelling system. *Geoscientific Model Development Discussions*, *4*(2), 223–253. https://doi.org/10.5194/gmd-4-223-2011

Hormann, V., & Brandt, P. (2007). Atlantic Equatorial Undercurrent and associated cold tongue variability. *Journal of Geophysical Research*, *112*(C6). https://doi.org/10.1029/2006JC003931

International Union for Conservation of Nature. (2023). The IUCN red list of threatened species. Retrieved from https://www.iucnredlist.org

Jackson, T., Sathyendranath, S., Groom, S., & Calton, B. (2022). ESA ocean colour climate change initiative – Phase 3: Product user guide for v6.0 Dataset (Tech. Rep.). Retrieved from https://docs.pml.space/share/s/fzNSPb4aQaSDvO7xBNOCIw

Jankowska, E., Pelc, R., Alvarez, J., Mehra, M., & Frischmann, C. J. (2022). Climate benefits from establishing marine protected areas targeted at blue carbon solutions. *Proceedings of the National Academy of Sciences*, *119*(23), e2121705119. https://doi.org/10.1073/pnas.2121705119

Jaureguiberry, P., Titeux, N., Wiemers, M., Bowler, D. E., Coscieme, L., Golden, A. S., et al. (2022). The direct drivers of recent global anthropogenic biodiversity loss. *Science Advances*, *8*(45), eabm9982. https://doi.org/10.1126/sciadv.abm9982

Jefferson, T., Costello, M. J., Zhao, Q., & Lundquist, C. J. (2021). Conserving threatened marine species and biodiversity requires 40% ocean protection. *Biological Conservation*, *264*, 109368. https://doi.org/10.1016/j.biocon.2021.109368

Jin, P., Hutchins, D. A., & Gao, K. (2020). The impacts of ocean acidification on marine food quality and its potential food chain consequences. *Frontiers in Marine Science*, *7*. https://doi.org/10.3389/fmars.2020.543979

Johns, W., Brandt, P., Bourlès, B., Tantet, A., Papapostolou, A., & Houk, A. (2014). Zonal structure and seasonal variability of the Atlantic equatorial undercurrent. *Climate Dynamics*, *43*(11), 3047–3069. https://doi.org/10.1007/s00382-014-2136-2

Johns, W., Speich, S., Araujo, M., Balmaseda, M., Chang, P., Dandin, P., et al. (2021). Tropical Atlantic Observing System (TAOS) review report (Vol. CLIVAR-01/2021; Tech. Rep.). Climate and Ocean - Variability, Predictability, and Change (CLIVAR) Atlantic Region Panel (ARP). https://doi.org/10.36071/clivar.rp.1.2021

Jones, C. D., Hughes, J. K., Bellouin, N., Hardiman, S. C., Jones, G. S., Knight, J., et al. (2011). The HadGEM2-ES implementation of CMIP5 centennial simulations. *Geoscientific Model Development*, *4*(3), 543–570. https://doi.org/10.5194/gmd-4-543-2011

Kraus, D. R., & Jackson, D. C. (1980). Temperature effects on ventilation and acid-base balance of the green turtle. *American Journal of Physiology - Regulatory, Integrative and Comparative Physiology*, *239*(3), R254–R258. https://doi.org/10.1152/ajpregu.1980.239.3.R254

Kwiatkowski, L., Torres, O., Bopp, L., Aumont, O., Chamberlain, M., Christian, J. R., et al. (2020). Twenty-first century ocean warming, acidification, deoxygenation, and upper-ocean nutrient and primary production decline from CMIP6 model projections. *Biogeosciences*, *17*(13), 3439–3470. https://doi.org/10.5194/bg-17-3439-2020

Lee, J.-Y., Marotzke, J., Bala, G., Cao, L., Corti, S., Dunne, J., et al. (2021). Future global climate: Scenario-based projections and near-term information [Book Section]. In V. Masson-Delmotte, et al. (Eds.), *Climate change 2021: The physical science basis. Contribution of working group i to the sixth assessment report of the intergovernmental panel on climate change* (pp. 553–672). https://doi.org/10.1017/9781009157896.006

Lellis, W. A., & Russell, J. A. (1990). Effect of temperature on survival, growth and feed intake of postlarval spiny lobsters, Panulirus argus. *Aquaculture*, *90*(1), 1–9. https://doi.org/10.1016/0044-8486(90)90277-T

Lindeque, P. K., Cole, M., Coppock, R. L., Lewis, C. N., Miller, R. Z., Watts, A. J., et al. (2020). Are we underestimating microplastic abundance in the marine environment? A comparison of microplastic capture with nets of different mesh-size. *Environmental Pollution*, *265*, 114721. https://doi.org/10.1016/j.envpol.2020.114721

Locarnini, R. A., Mishonov, A. V., Baranova, O. K., Boyer, T. P., Zweng, M. M., Garcia, H. E., et al. (2018). World Ocean Atlas 2018, Volume 1: Temperature (Vol. 81; Report). Retrieved from https://archimer.ifremer.fr/doc/00651/76337/

Lotze, H. K., Tittensor, D. P., Bryndum-Buchholz, A., Eddy, T. D., Cheung, W. W. L., Galbraith, E. D., et al. (2019). Global ensemble projections reveal trophic amplification of ocean biomass declines with climate change. *Proceedings of the National Academy of Sciences*, *116*(26), 12907–12912. https://doi.org/10.1073/pnas.1900194116

Maina, G., Osuka, K., & Samoilys, M. (2011). Opportunities and challenges of community-based marine protected areas in Kenya. CORDIO Status Report.

Mariani, G., Cheung, W. W. L., Lyet, A., Sala, E., Mayorga, J., Velez, L., et al. (2020). Let more big fish sink: Fisheries prevent blue carbon sequestration—Half in unprofitable areas. *Science Advances*, *6*(44), eabb4848. https://doi.org/10.1126/sciadv.abb4848

Marine Conservation Institute. (2023). The marine protection atlas. Retrieved from https://mpatlas.org/

Marshall, L. R., Maters, E. C., Schmidt, A., Timmreck, C., Robock, A., & Toohey, M. (2022). Volcanic effects on climate: Recent advances and future avenues. *Bulletin of Volcanology*, *84*(5), 54. https://doi.org/10.1007/s00445-022-01559-3

Martin, S., & Gattuso, J.-P. (2009). Response of Mediterranean coralline algae to ocean acidification and elevated temperature. *Global Change Biology*, *15*(8), 2089–2100. https://doi.org/10.1111/j.1365-2486.2009.01874.x

McCoy, S. J., & Kamenos, N. A. (2015). Coralline algae (Rhodophyta) in a changing world: Integrating ecological, physiological, and geochemical responses to global change. *Journal of Phycology*, *51*(1), 6–24. https://doi.org/10.1111/jpy.12262

McDonald, B. (2012). Ascension Island shore fishing. https://planetseafishing.com/features/ascension-island-shore-fishing/

Montes, E., Muller-Karger, F. E., Cianca, A., Lomas, M. W., Lorenzoni, L., & Habtes, S. (2016). Decadal variability in the oxygeninventory of North Atlantic subtropicalunderwater captured by sustained, long-term oceanographic time seriesobservations. *Global Biogeochemical Cycles*, *30*(3), 460–478. https://doi.org/10.1002/2015GB005183

Nowicki, M., DeVries, T., & Siegel, D. A. (2022). Quantifying the carbon export and sequestration pathways of the ocean's biological carbon pump. *Global Biogeochemical Cycles*, *36*(3), e2021GB007083. https://doi.org/10.1029/2021GB007083

Oldfield, S., Procter, D., & Fleming, L. (1999). *Biodiversity: The UK overseas territories* (Tech. Rep.). United Kingdom Overseas Territories Project.

O'Leary, B. C., Winther-Janson, M., Bainbridge, J. M., Aitken, J., Hawkins, J. P., & Roberts, C. M. (2016). Effective coverage targets for ocean protection. *Conservation Letters*, *9*(6), 398–404. https://doi.org/10.1111/conl.12247

Olsen, A., Key, R. M., van Heuven, S., Lauvset, S. K., Velo, A., Lin, X., et al. (2016). The Global Ocean Data Analysis Project Version 2 (GLODAPv2) - An internally consistent data product for the world ocean. *Earth System Science Data*, *8*(2), 297–323. https://doi.org/10.5194/essd-8-297-2016

O'Neill, B. C., Tebaldi, C., van Vuuren, D. P., Eyring, V., Friedlingstein, P., Hurtt, G., et al. (2016). The scenario model intercomparison project (ScenarioMIP) for CMIP6. *Geoscientific Model Development*, *9*(9), 3461–3482. https://doi.org/10.5194/gmd-9-3461-2016

O'Regan, S. M., Archer, S. K., Friesen, S. K., & Hunter, K. L. (2021). A global assessment of climate change adaptation in marine protected area management plans. *Frontiers in Marine Science*, *8*. https://doi.org/10.3389/fmars.2021.711085

Oschlies, A., Brandt, P., Stramma, L., & Schmidtko, S. (2018). Drivers and mechanisms of ocean deoxygenation. *Nature Geoscience*, *11*(7), 467–473. https://doi.org/10.1038/s41561-018-0152-2

Parker, L. M., Ross, P. M., O'Connor, W. A., Pörtner, H. O., Scanes, E., & Wright, J. M. (2013). Predicting the response of molluscs to the impact of ocean acidification. *Biology*, *2*(2), 651–692. https://doi.org/10.3390/biology2020651

Petrie, R., Denvil, S., Ames, S., Levavasseur, G., Fiore, S., Allen, C., et al. (2021). Coordinating an operational data distribution network for CMIP6 data. *Geoscientific Model Development*, *14*(1), 629–644. https://doi.org/10.5194/gmd-14-629-2021

Petrik, C. M., Luo, J. Y., Heneghan, R. F., Everett, J. D., Harrison, C. S., & Richardson, A. J. (2022). Assessment and constraint of meso-zooplankton in CMIP6 earth system models. *Global Biogeochemical Cycles*, *36*(11), e2022GB007367. https://doi.org/10.1029/2022GB007367

Pikitch, E. K. (2012). The risks of overfishing. *Science*, *338*(6106), 474–475. https://doi.org/10.1126/science.1229965

Pimiento, C., Leprieur, F., Silvestro, D., Lefcheck, J. S., Albouy, C., Rasher, D. B., et al. (2020). Functional diversity of marine megafauna in the anthropocene. *Science Advances*, *6*(16), eaay7650. https://doi.org/10.1126/sciadv.aay7650

Polimene, L., Sailley, S., Clark, D., Mitra, A., & Allen, J. I. (2016). Biological or microbial carbon pump? The role of phytoplankton stoichiometry in ocean carbon sequestration. *Journal of Plankton Research*, *39*(2), 180–186. https://doi.org/10.1093/plankt/fbw091

Poloczanska, E. S., Burrows, M. T., Brown, C. J., García Molinos, J., Halpern, B. S., Hoegh-Guldberg, O., et al. (2016). Responses of marine organisms to climate change across oceans. *Frontiers in Marine Science*, *3*. https://doi.org/10.3389/fmars.2016.00062

Poloczanska, E. S., Limpus, C. J., & Hays, G. C. (2009). Chapter 2 vulnerability of marine turtles to climate change. In *Advances in marine biology* (Vol. 56, pp. 151–211). Academic Press. https://doi.org/10.1016/S0065-2881(09)56002-6

Price, J., & John, D. (1980). Ascension Island, South Atlantic: A survey of inshore benthic macroorganisms, communities and interactions. *Aquatic Botany*, *9*, 251–278. https://doi.org/10.1016/0304-3770(80)90026-1

Qiu, Z., Qiao, F., Jang, C. J., Zhang, L., & Song, Z. (2021). Evaluation and projection of global marine heatwaves based on CMIP6 models. *Deep Sea Research Part II: Topical Studies in Oceanography*, *194*, 104998. https://doi.org/10.1016/j.dsr2.2021.104998

Queirós, A. M., Talbot, E., Beaumont, N. J., Somerfield, P. J., Kay, S., Pascoe, C., et al. (2021). Bright spots as climate-smart marine spatial planning tools for conservation and blue growth. *Global Change Biology*, *27*(21), 5514–5531. https://doi.org/10.1111/gcb.15827

Ragazzola, F., Foster, L. C., Form, A., Anderson, P. S., Hansteen, T. H., & Fietzke, J. (2012). Ocean acidification weakens the structural integrity of coralline algae. *Global Change Biology*, *18*(9), 2804–2812. https://doi.org/10.1111/j.1365-2486.2012.02756.x

Rees, A. P., Smyth, T. J., & Brotas, V. (2024). Editorial: The Atlantic meridional transect programme (1995-2023). *Frontiers in Marine Science*, *11*. https://doi.org/10.3389/fmars.2024.1358174

Riahi, K., van Vuuren, D. P., Kriegler, E., Edmonds, J., O'Neill, B. C., Fujimori, S., et al. (2017). The Shared Socioeconomic Pathways and their energy, land use, and greenhouse gas emissions implications: An overview. *Global Environmental Change*, *42*, 153–168. https://doi.org/10.1016/j.gloenvcha.2016.05.009

Richardson, A. J., Downes, K. J., Nolan, E. T., Brickle, P., Brown, J., Weber, N., & Weber, S. B. (2018). Residency and reproductive status of yellowfin tuna in a proposed large-scale pelagic marine protected area. *Aquatic Conservation: Marine and Freshwater Ecosystems*, *28*(6), 1308–1316. https://doi.org/10.1002/aqc.2936

Richter, I., & Tokinaga, H. (2022). An overview of the performance of CMIP6 models in the tropical Atlantic: Mean state, variability, and remote impacts. *Climate Dynamics*, *55*(9–10), 2579–2601. https://doi.org/10.1007/s00382-020-05409-w

Righi, M., Andela, B., Eyring, V., Lauer, A., Predoi, V., Schlund, M., et al. (2020). Earth system model evaluation tool (ESMValTool) v2.0 - Technical overview. *Geoscientific Model Development*, *13*(3), 1179–1199. https://doi.org/10.5194/gmd-13-1179-2020

Robinson, D. P., Jaidah, M. Y., Bach, S. S., Rohner, C. A., Jabado, R. W., Ormond, R., & Pierce, S. J. (2017). Some like it hot: Repeat migration and residency of whale sharks within an extreme natural environment. *PLoS One*, *12*(9), 1–23. https://doi.org/10.1371/journal.pone.0185360

Rodolfo-Metalpa, R., Houlbrèque, F., Tambutté, É., Boisson, F., Baggini, C., Patti, F. P., et al. (2011). Coral and mollusc resistance to ocean acidification adversely affected by warming. *Nature Climate Change*, *1*(6), 308–312. https://doi.org/10.1038/nclimate1200

Rohr, T., Richardson, A. J., Lenton, A., Chamberlain, M. A., & Shadwick, E. H. (2023). Zooplankton grazing is the largest source of uncertainty for marine carbon cycling in CMIP6 models. *Communications Earth & Environment*, *4*(1), 212. https://doi.org/10.1038/s43247-023-00871-w

Roleda, M. Y., Cornwall, C. E., Feng, Y., McGraw, C. M., Smith, A. M., & Hurd, C. L. (2015). Effect of ocean acidification and pH fluctuations on the growth and development of coralline algal recruits, and an associated benthic algal assemblage. *PLoS One*, *10*(10), 1–19. https://doi.org/10.1371/journal.pone.0140394

Roman, J., & McCarthy, J. J. (2010). The whale pump: Marine mammals enhance primary productivity in a coastal basin. *PLoS One*, *5*(10), 1–8. https://doi.org/10.1371/journal.pone.0013255

Ross, E., & Behringer, D. (2019). Changes in temperature, pH, and salinity affect the sheltering responses of Caribbean spiny lobsters to chemosensory cues. *Scientific Reports*, *9*(1), 4375. https://doi.org/10.1038/s41598-019-40832-y

Royal Air Force. (2023). South Atlantic airbridge via Ascension Island base (Tech. Rep.). Retrieved from https://www.raf.mod.uk/our-organisation/stations/mount-pleasant-complex/flights-via-ascension-island/

Sala, E., Mayorga, J., Bradley, D., Cabral, R. B., Atwood, T. B., Auber, A., et al. (2021). Protecting the global ocean for biodiversity, food and climate. *Nature*, *592*(7854), 397–402. https://doi.org/10.1038/s41586-021-03371-z

Sathyendranath, S., Brewin, R. J., Brockmann, C., Brotas, V., Calton, B., Chuprin, A., et al. (2019). An ocean-colour time series for use in climate studies: The experience of the ocean-colour climate change initiative (OC-CCI). *Sensors*, *19*(19), 4285. https://doi.org/10.3390/s19194285

Schmidtko, S., Stramma, L., & Visbeck, M. (2017). Decline in global oceanic oxygen content during the past five decades. *Nature*, *542*(7641), 335–339. https://doi.org/10.1038/nature21399

Séférian, R., Berthet, S., Yool, A., Palmiéri, J., Bopp, L., Tagliabue, A., et al. (2020). Tracking improvement in simulated marine biogeochemistry between CMIP5 and CMIP6. *Current Climate Change Reports*, *6*(3), 95–119. https://doi.org/10.1007/s40641-020-00160-0

Sellar, A. A., Walton, J., Jones, C. G., Wood, R., Abraham, N. L., Andrejczuk, M., et al. (2020). Implementation of U.K. Earth system models for CMIP6. *Journal of Advances in Modeling Earth Systems*, *12*(4), e2019MS001946. https://doi.org/10.1029/2019MS001946

Smith, A. M. (2009). Bryozoans as southern sentinels of ocean acidification: A major role for a minor phylum. *Marine and Freshwater Research*, *60*(5), 475–482. https://doi.org/10.1071/MF08321

St Helena Goverment. (2023). St Helena's Marine protected area. Retrieved from https://www.sainthelena.gov.sh/2016/public-announcements/st-helenas-marine-protected-area/

Stramma, L., Prince, E. D., Schmidtko, S., Luo, J., Hoolihan, J. P., Visbeck, M., et al. (2012). Expansion of oxygen minimum zones may reduce available habitat for tropical pelagic fishes. *Nature Climate Change*, *2*(1), 33–37. https://doi.org/10.1038/NCLIMATE1304

Sukhdev, P., Wittmer, H., Schröter-Schlaack, C., Nesshöver, C., Bishop, J., ten Brink, P., et al. (2010). *The economics of ecosystems and biodiversity: Mainstreaming the economics of nature: A synthesis of the approach, conclusions and recommendations of TEEB* (Tech. Rep.). The Economics of Ecosystems and Biodiversity.

Tagliabue, A., Kwiatkowski, L., Bopp, L., Butenschön, M., Cheung, W., Lengaigne, M., & Vialard, J. (2021). Persistent uncertainties in ocean net primary production climate change projections at regional scales raise challenges for assessing impacts on ecosystem services. *Frontiers in Climate*, *3*. https://doi.org/10.3389/fclim.2021.738224

Tebaldi, C., Debeire, K., Eyring, V., Fischer, E., Fyfe, J., Friedlingstein, P., et al. (2021). Climate model projections from the scenario model intercomparison project (ScenarioMIP) of CMIP6. *Earth System Dynamics*, *12*(1), 253–293. https://doi.org/10.5194/esd-12-253-2021

Thompson, C. D. H., Meeuwig, J. J., Brown, J., Richardson, A. J., Friedlander, A. M., Miller, P. I., & Weber, S. B. (2021). Spatial variation in pelagic wildlife assemblages in the Ascension Island marine protected area: Implications for monitoring and management. *Frontiers in Marine Science*, *8*. https://doi.org/10.3389/fmars.2021.634599

Tilley, D., Ball, S., Ellick, J., Godley, B. J., Weber, N., Weber, S. B., & Broderick, A. C. (2019). No evidence of fine scale thermal adaptation in green turtles. *Journal of Experimental Marine Biology and Ecology*, *514–515*, 110–117. https://doi.org/10.1016/j.jembe.2019.04.001

Tittensor, D. P., Beger, M., Boerder, K., Boyce, D. G., Cavanagh, R. D., Cosandey-Godin, A., et al. (2019). Integrating climate adaptation and biodiversity conservation in the global ocean. *Science Advances*, *5*(11), eaay9969. https://doi.org/10.1126/sciadv.aay9969

Tittensor, D. P., Eddy, T. D., Lotze, H. K., Galbraith, E. D., Cheung, W., Barange, M., et al. (2018). A protocol for the intercomparison of marine fishery and ecosystem models: Fish-MIP v1.0. *Geoscientific Model Development*, *11*(4), 1421–1442. https://doi.org/10.5194/gmd-11-1421-2018

Tittensor, D. P., Novaglio, C., Harrison, C. S., Heneghan, R. F., Barrier, N., Bianchi, D., et al. (2021). Next-generation ensemble projections reveal higher climate risks for marine ecosystems. *Nature Climate Change*, *11*(11), 973–981. https://doi.org/10.1038/s41558-021-01173-9

Tokinaga, H., & Xie, S.-P. (2011). Weakening of the equatorial Atlantic cold tongue over the past six decades. *Nature Geoscience*, *4*(4), 222–226. https://doi.org/10.1038/ngeo1078

Townhill, B. L., Couce, E., Bell, J., Reeves, S., & Yates, O. (2021). Climate change impacts on Atlantic oceanic island tuna fisheries. *Frontiers in Marine Science*, *8*. https://doi.org/10.3389/fmars.2021.634280

Trevathan-Tackett, S. M., Kelleway, J., Macreadie, P. I., Beardall, J., Ralph, P., & Bellgrove, A. (2015). Comparison of marine macrophytes for their contributions to blue carbon sequestration. *Ecology*, *96*(11), 3043–3057. https://doi.org/10.1890/15-0149.1

Tsiamis, K., Peters, A. F., Shewring, D. M., Asensi, A. O., Van West, P., & Küpper, F. C. (2017). Marine benthic algal flora of Ascension Island, South Atlantic. *Journal of the Marine Biological Association of the United Kingdom*, *97*(4), 681–688. https://doi.org/10.1017/S0025315414000952

Turner, J. T. (2015). Zooplankton fecal pellets, marine snow, phytodetritus and the ocean's biological pump. *Progress in Oceanography*, *130*, 205–248. https://doi.org/10.1016/j.pocean.2014.08.005

United Nations General Assembly. (2017). International legally binding instrument under the United Nations Convention on the Law of the Sea on the conservation and sustainable use of marine biological diversity of areas beyond national jurisdiction (Vol. *Resolution 72/249*). Retrieved from https://documents-dds-ny.un.org/doc/UNDOC/GEN/N17/468/77/PDF/N1746877.pdf?OpenElemen

Uy, T., Fitzgibbon, Q. P., Codabaccus, B. M., & Smith, G. G. (2023). Thermal physiology of tropical rock lobster (Panulirus ornatus); defining physiological constraints to high temperature tolerance. *Aquaculture*, *569*, 739357. https://doi.org/10.1016/j.aquaculture.2023.739357

Vichi, M., Lovato, T., Lazzari, P., Cossarini, G., Gutierrez Mlot, E., Mattia, G., et al. (2015). The biogeochemical flux model (BFM): Equation description and user manual. BFM version 5.1. Release 1.1 (Tech. Rep.). https://doi.org/10.13140/RG.2.1.2176.9444

Watson, R. T., & Zakri, A. H. (2005). Ecosystems and human well-being: Opportunities and challenges for business and industry.

Watson, S.-A., Southgate, P., Miller, G., Moorhead, J., & Knauer, J. (2012). Ocean acidification and warming reduce juvenile survival of the fluted giant clam, Tridacna squamosa. *Molluscan Research*, *32*(3), 177–180. https://doi.org/10.11646/mr.32.3.7

Weber, S., Lambdon, P., & Baum, D. (2023). Climate resilience and conservation of Ascension's biodiversity (CRACAB) project final report (Tech. Rep.). Retrieved from https://darwinplus.org.uk/documents/DPLUS113/26801/DPLUS113 FR - edited.pdf

Weber, S. B., & Weber, N. (2019). Important bird areas: Ascension island. *British Birds*, *112*(11), 661–682-3018.

Weber, S. B., Weber, N., Ellick, J., Avery, A., Frauenstein, R., Godley, B. J., et al. (2014). Recovery of the South Atlantic's largest green turtle nesting population. *Biodiversity & Conservation*, *23*(12), 3005–3018. https://doi.org/10.1007/s10531-014-0759-6

Weijer, W., Cheng, W., Garuba, O. A., Hu, A., & Nadiga, B. T. (2020). CMIP6 models predict significant 21st century decline of the Atlantic meridional overturning circulation. *Geophysical Research Letters*, *47*(12), e2019GL086075. https://doi.org/10.1029/2019GL086075

Whitfield, M. (1975). The effect of increases in the atmospheric carbon dioxide content on the carbonate ion concentration of surface ocean water at 25°C. *Limnology & Oceanography*, *20*(1), 103–108. https://doi.org/10.4319/lo.1975.20.1.0103

Wilson, K. L., Tittensor, D. P., Worm, B., & Lotze, H. K. (2020). Incorporating climate change adaptation into marine protected area planning. *Global Change Biology*, *26*(6), 3251–3267. https://doi.org/10.1111/gcb.15094

Wirtz, P., Bingeman, J., Bingeman, J., Fricke, R., Hook, T. J., & Young, J. (2017). The fishes of Ascension Island, central Atlantic Ocean – New records and an annotated checklist. *Journal of the Marine Biological Association of the United Kingdom*, *97*(4), 783–798. https://doi.org/10.1017/S0025315414001301

Woodley, S., Locke, H., Laffoley, D., MacKinnon, K., Sandwith, T., & Smart, J. (2019). A review of evidence for area-based conservation targets for the post-2020 global biodiversity framework. *PARKS*(25.2), 31–46. https://doi.org/10.2305/IUCN.CH.2019.PARKS-25-2SW2.en

Yao, Y.-T., Du, Y., Pan, J.-X., Lin, C.-X., Ji, X., & You, W.-H. (2022). Incubating green turtle (Chelonia mydas) eggs at constant temperatures: Hatching success, hatchling morphology and post-hatch growth. *Journal of Thermal Biology*, *104*, 103182. https://doi.org/10.1016/j.jtherbio.2021.103182

Yool, A., Palmiéri, J., Jones, C. G., Sellar, A. A., de Mora, L., Kuhlbrodt, T., et al. (2020). Spin-up of UK earth system model 1 (UKESM1) for CMIP6. *Journal of Advances in Modeling Earth Systems*, *12*(8), e2019MS001933. https://doi.org/10.1029/2019MS001933

Zweng, M. M., Reagan, J. R., Seidov, D., Boyer, T. P., Locarnini, R. A., Garcia, H. E., et al. (2018). World Ocean Atlas 2018, Volume 2: Salinity (Vol. 82; Report). Retrieved from https://archimer.ifremer.fr/doc/00651/76337/